Doa1 targets ubiquitinated substrates for mitochondria-associated degradation

Xi Wu, Lanlan Li, and Hui Jiang

National Institute of Biological Sciences, Beijing 102206, China

Mitochondria-associated degradation (MAD) mediated by the Cdc48 complex and proteasome degrades ubiquitinated mitochondrial outer-membrane proteins. MAD is critical for mitochondrial proteostasis, but it remains poorly characterized. We identified several mitochondrial Cdc48 substrates and developed a genetic screen assay to uncover regulators of the Cdc48-dependent MAD pathway. Surprisingly, we identified Doa1, a substrate-processing factor of Cdc48 that inhibits the degradation of some Cdc48 substrates, as a critical mediator of the turnover of mitochondrial Cdc48 substrates. Deletion of *DOA1* causes the accumulation and mislocalization of substrates on mitochondria. Profiling of Cdc48 cofactors shows that Doa1 and Cdc48$^{\text{-Ufd1-Npl4}}$ form a functional complex mediating MAD. Biochemically, Doa1 interacts with ubiquitinated substrates and facilitates substrate recruitment to the Cdc48$^{\text{-Ufd1-Npl4}}$ complex. Functionally, Doa1 is critical for cell survival under mitochondrial oxidative stress, but not ER stress, conditions. Collectively, our results demonstrate the essential role of the Doa1–Cdc48$^{\text{-Ufd1-Npl4}}$ complex in mitochondrial proteostasis and suggest that Doa1 plays dual roles on the Cdc48 complex.

Introduction

Owing to their essential metabolic and signaling functions, mitochondria are under close surveillance by complex quality-control mechanisms, including reactive oxygen species removal by anti-oxidation enzymes (Collins et al., 2012), intra-mitochondrial protein turnover by mitochondrial proteases (Quirós et al., 2015), mitophagy (Youle and Narendra, 2011), and the mitochondria-associated degradation (MAD) pathway degrading mitochondrial outer-membrane (MOM) proteins (Karbowski and Youle, 2011; Taylor and Rutter, 2011).

MAD is analogous to the well-studied ER associated degradation (ERAD) pathway (Hirsch et al., 2009) in that they both require the highly conserved AAA-ATPase Cdc48 (TER94 in *Drosophila melanogaster* and VCP or p97 in mammals) to dislodge ubiquitinated proteins from organelle membranes and escort their degradation by the proteasome (Karbowski and Youle, 2011; Taylor and Rutter, 2011; Xu et al., 2011). Cdc48 forms a hexameric ring-like structure to unfold or remodel substrates and is extensively involved in cytoplasmic, nuclear, and organellar protein degradation, autophagy, and intracellular trafficking processes (Meyer et al., 2012). The cellular functions of Cdc48 are regulated by two types of cofactors: the substrate-recruiting factors that contain ubiquitin-binding domains to recognize and recruit ubiquitinated substrates to Cdc48, and the substrate-processing factors that often possess enzymatic activities to modulate the turnover rate of the Cdc48-bound substrates (Stolz et al., 2011; Meyer et al., 2012; Baek et al., 2013; Buchberger, 2013).

Accumulating evidence suggests that Cdc48 has an essential and evolutionarily conserved role in mitochondrial quality control. Cdc48/TER94/VCP mutations in yeast (Braun et al., 2006), *Drosophila* (Chang et al., 2011; Kim et al., 2013), mouse (Custer et al., 2010; Nalbandian et al., 2012; Yin et al., 2012), and human (Bartolome et al., 2013) all cause severe abnormalities in mitochondria, including mitochondrial swelling and aggregation, production of reactive oxygen species, and reduced ATP production. Pathogenic mutations of human VCP cause several muscular and neural degenerative diseases (Watts et al., 2004; Johnson et al., 2010).

Although the importance of the Cdc48-dependent MAD pathway is being increasingly appreciated, its molecular mechanism remains obscure. First, only a very limited number of mitochondrial Cdc48 substrates have been reported; these include Fzo1 (Cohen et al., 2008; Heo et al., 2010) in yeast and mitofusins (Tanaka et al., 2010; Xu et al., 2011) and Mcl-1 (Xu et al., 2011) in mammals. Second, the regulatory components of MAD remain largely unknown. It has been proposed that in yeast, MAD is mediated by the Vms1–Npl4–Cdc48 complex, in which Npl4 may interact with ubiquitinated substrates (Heo et al., 2010). However, it is noteworthy that the ubiquitin-binding

Correspondence to Hui Jiang: jianghui@nibs.ac.cn; or Xi Wu: wuxi@nibs.ac.cn

Abbreviations used in this paper: CHX, cycloheximide; ERAD, ER-associated degradation; ERMES, ER–mitochondria encounter structure; G6PDH, glucose-6-phosphate dehydrogenase; IP, immunoprecipitation; MAD, mitochondria-associated degradation; MOM, mitochondrial outer membrane; PMS, postmitochondria supernatant; ts, temperature sensitive; Ub, ubiquitin; UBD, ubiquitin-binding domain; UPR, unfolded protein response; WCE, whole-cell extract.

The Rockefeller University Press $30.00
J. Cell Biol. Vol. 213 No. 1 49–63
www.jcb.org/cgi/doi/10.1083/jcb.201510098

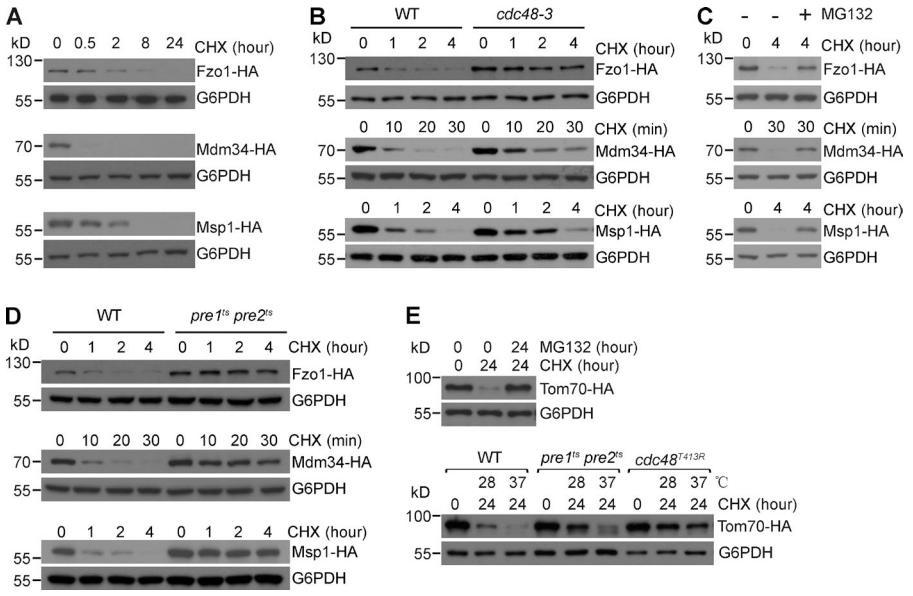

Figure 1. **Identification of mitochondrial Cdc48 substrates.** If not otherwise indicated, all the tagged proteins depicted in this and other figures were expressed from the endogenous chromosomal loci. (A) The *FZO1-HA*, *MDM34-HA*, and *MSP1-HA* strains were grown to log phase and then treated with cycloheximide (CHX) and collected at the indicated time points. Anti-G6PDH blots are shown as loading controls. (B) The *FZO1-HA*, *MDM34-HA*, and *MSP1-HA* strains in wild-type (WT) or *cdc48-3* background were grown to log phase at 25°C and then treated with CHX at 28°C (semirestrictive temperature). (C) The *FZO1-HA*, *MDM34-HA*, and *MSP1-HA* strains were grown to log phase and then treated with CHX alone or CHX + MG132 as indicated. (D) The *FZO1-HA*, *MDM34-HA*, and *MSP1-HA* strains in WT or *pre1*^{ts} *pre2*^{ts} background were treated as in B. (E) The *TOM70-HA* CEN.PK strain was grown to log phase and then treated with CHX and MG132 as indicated (top). The *TOM70-HA* CEN.PK strains in WT, *pre1*^{ts} *pre2*^{ts}, or *cdc48*^{T413R} background were grown to log phase at 25°C and then treated with CHX at 28°C or at 37°C (restrictive temperature; bottom).

NZF domain present in mammalian Npl4 is not conserved in yeast Npl4 (Meyer et al., 2002; Ye et al., 2003), and yeast Npl4 was not classified as a ubiquitin-binding protein (Stolz et al., 2011; Buchberger, 2013). The involvement of Vms1 in MAD has been supported by its requirement for Fzo1 degradation (Heo et al., 2010), but the role of Vms1 in Fzo1 turnover has been debated (Esaki and Ogura, 2012).

To investigate the molecular mechanisms and biological functions of the Cdc48-dependent MAD pathway, we analyzed the turnover of transmembrane MOM proteins and identified mitochondrial Cdc48 substrates in *Saccharomyces cerevisiae*. The newly identified substrates allowed us to establish a genetic screen to identify MAD regulators and characterize their roles in mitochondrial proteostasis and mitochondrial quality control.

Results

Identification of mitochondrial Cdc48 substrates

To identify mitochondrial Cdc48 substrates, we tagged transmembrane MOM proteins by chromosomal integration with a HA tag (6xHA at the C terminus or 3xHA at the N terminus) and analyzed their turnover. To minimize potential artifacts, we focused on the experimentally verified transmembrane MOM proteins whose mitochondrial localization and functions are not affected by epitope tags (Table S1 and supplemental references therein). We tested 18 such proteins and successfully generated 14 strains that had normal growth and detectable HA signals on Western blot (Table S1). We monitored the degradation of these HA-tagged proteins after stopping new protein synthesis with cycloheximide (CHX) treatment, and we identified nine slow-turnover proteins (Fig. S1 A) and five fast-turnover proteins (Figs. 1 A and S1 B).

We inactivated the Cdc48-proteasome pathway by using the widely used temperature-sensitive (ts) mutants of Cdc48 (*cdc48-3*) and proteasome (*pre1*^{ts} *pre2*^{ts}). Among the five fast-turnover proteins, the degradation of Fzo1-HA, Mdm34-HA, and Msp1-HA was inhibited by ts inactivation of Cdc48 and proteasome and by the proteasome inhibitor MG132 (Fig. 1, B–D). The degradation of the other two proteins (Tom22-HA and Om45-HA) was not inhibited in the *cdc48-3* or the *pre1*^{ts} *pre2*^{ts} mutants (Fig. S1 C). The degradation of all the five proteins was insensitive to the deletion of the autophagy regulator *ATG5* (Fig. S1 D) or the vacuolar proteases *PEP4* and *PRB1* (Fig. S1 E). Therefore, we confirmed Fzo1-HA, Mdm34-HA, and Msp1-HA as Cdc48 substrates. We further did imaging and growth tests to confirm that C-terminal tagging of the three Cdc48 substrates does not affect their localization (Fig. S1 F) or cell growth (Fig. S1 G).

The aforementioned characterization of MOM proteins was conducted in the BY4741 strain. The MOM protein Tom70 was long-lived (Fig. S1 A) in the BY4741 strain but had a fast turnover rate (Fig. 1 E) in the prototrophic CEN.PK strain (van Dijken et al., 2000). The degradation of Tom70-HA was inhibited in the ts mutants of proteasome (*pre1*^{ts} *pre2*^{ts}) and Cdc48 (*cdc48*^{T413R}; Fig. 1 E). Therefore, Tom70-HA is another Cdc48 substrate in the CEN.PK strain.

A genetic screen identifies MAD regulators

To identify the regulatory components of the Cdc48-dependent MAD pathway, we need a simple and efficient way to monitor the turnover of substrates on a large scale. We thus developed a colony assay for such a purpose (Fig. S2 A) and tested the four substrates (Fzo1-HA, Mdm34-HA, Msp1-HA, and Tom70-HA) with this assay. Among the four substrates, we observed an almost complete loss of Tom70-HA signal after CHX treatment, and the degradation of Tom70-HA was blocked by knocking down *CIM3*, a proteasome subunit (Fig. S2 B). We therefore performed a transposon-based insertion screen using Tom70-HA as the reporter substrate (Fig. 2 A).

We screened ∼5,000 colonies, covering ∼15% of the genome, and identified insertional mutations in 16 genes (Table S2). Among these putative hits, we found four genes related to the Cdc48-proteasome pathway. These genes are *DOA1* (a Cdc48 cofactor; Johnson et al., 1995; Ghislain et al., 1996),

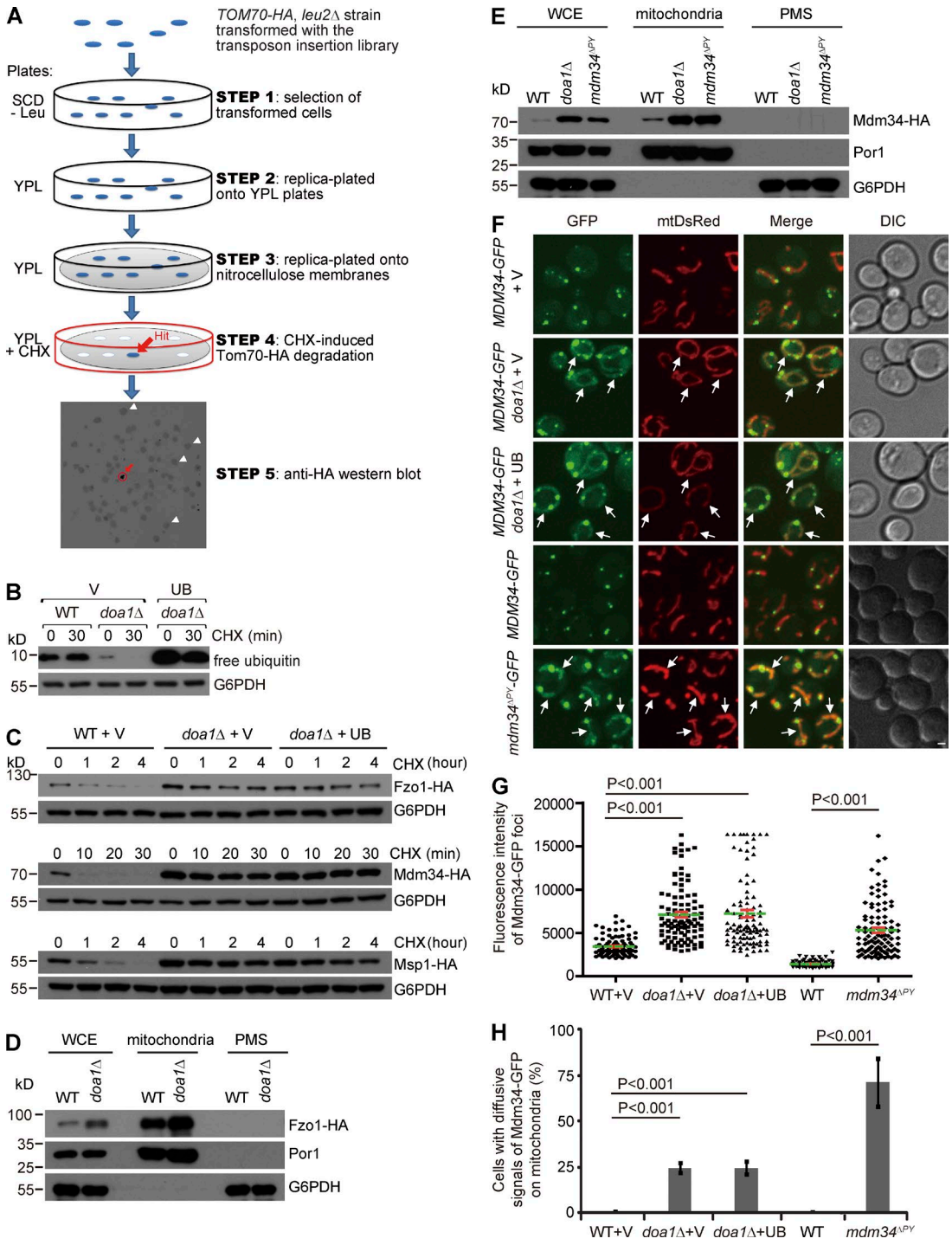

Figure 2. **Doa1 mediates the turnover of mitochondrial Cdc48 substrates, and deletion of *DOA1* causes substrate accumulation and mislocalization on mitochondria.** (A) Schematic illustration of the colony screen assay (see Materials and methods for details). Blue indicates Tom70-HA signal. In the representative Western blot image, white arrowheads point to colonies with normal degradation of Tom70-HA, and the red arrow points to a colony defective in Tom70-HA degradation. (B) The WT and *doa1Δ* strains transformed with a high-copy plasmid expressing ubiquitin (UB) or the empty vector (V) were grown to log phase before CHX treatment. (C) The *FZO1-HA*, *MDM34-HA*, and *MSP1-HA* strains in WT or *doa1Δ* background were transformed with V or UB plasmids and grown to log phase before CHX treatment. (D) Subcellular fractionation of the *FZO1-HA* and *FZO1-HA doa1Δ* strains. Lysates from the whole-cell extracts (WCEs), mitochondria-enriched fraction, and postmitochondria supernatant (PMS) were analyzed by Western blot. G6PDH and Por1 are the markers for cytoplasm and mitochondria, respectively. (E) Subcellular fractionation of the *MDM34-HA*, *MDM34-HA doa1Δ*, and *mdm34$^{\Delta PY}$-HA* strains were analyzed as in D. (F) The indicated WT or mutant strains chromosomally expressing Mdm34-GFP and mtDsRed (labeling mitochondria) were grown in glucose media to log phase before imaging. Z projections and differential interference contrast images are shown. Bar, 1 µm. White arrows point to diffusive mitochondrial signals of Mdm34-GFP. (G) Quantitative analysis of the foci intensity of Mdm34-GFP. Data values represent means (green line) ± SEM (red line). *n* = 100 for each strain. Similar results were obtained in two additional, independent experiments. Data were analyzed by one-way analysis of variance followed by Tukey post tests. (H) Quantitative analysis of the percentage of cells with diffusive mitochondrial signals of Mdm34-GFP. Data values represent means ± SEM from three independent experiments, with at least 200 cells counted in each experiment. Data were analyzed by one-way analysis of variance followed by Tukey post tests. Note that ubiquitin overexpression did not rescue the increased foci intensity or the mislocalization phenotype of Mdm34-GFP in *doa1Δ* cells.

UBP6 (a proteasome-associated ubiquitin protease; Verma et al., 2000), *BRO1* (associated with deubiquitinase Doa4; Luhtala and Odorizzi, 2004), and *RSP5* (an E3 ubiquitin ligase; Huibregtse et al., 1995). Deletions of *BRO1*, *UBP6*, and ts inactivation of Rsp5 inhibited the degradation of Tom70-HA, Mdm34-HA, and Msp1-HA, but not that of Fzo1-HA (Fig. S2, C and E–G). In contrast, deletion of *DOA1* inhibited the degradation of all the four substrates (Fig. S2, C and D).

Mdm34 has a highly conserved PY motif, PPPY, at its C terminus (Fig. S2 H), which has been shown to mediate the interaction between Rsp5 and its substrates (Rotin and Kumar, 2009). Consistently, the PPPY to AAAA (mdm34$^{\Delta PY}$) mutation strongly blocked Mdm34-HA degradation and elevated its steady level (Fig. S2 I), demonstrating that Mdm34 is a bona fide Rsp5 substrate.

Doa1 (also known as Ufd3) is a Cdc48 cofactor known for two decades (Johnson et al., 1995; Ghislain et al., 1996) and was reported to function as a substrate-processing factor (Rumpf and Jentsch, 2006). Another substrate-processing factor, Ufd2, catalyzes the ubiquitination of some Cdc48-bound substrates and promotes their degradation (Koegl et al., 1999; Rumpf and Jentsch, 2006). Doa1 competes with Ufd2 for the same binding site on Cdc48 and thus inhibits the degradation of the Ufd2-dependent substrates (Rumpf and Jentsch, 2006). Apparently, our results cannot be explained by the substrate-processing function of Doa1.

It is also known that deletion of *DOA1* reduces free ubiquitin level and thus indirectly inhibits the degradation of some proteins, such as Ubi-Pro–β-galactosidase; ubiquitin overexpression rescues the protein degradation defects of *doa1Δ* cells (Johnson et al., 1995). As reported, the *doa1Δ* cells had reduced ubiquitin level, which was rescued by ubiquitin overexpression (Johnson et al., 1995; Fig. 2 B) or by the deletion of *UFD2* (Rumpf and Jentsch, 2006; Fig. S2 J). Surprisingly, the impaired degradation of mitochondrial Cdc48 substrates (Fzo1-HA, Mdm34-HA, and Msp1-HA) was not rescued by restoring the ubiquitin level (Figs. 2 C and S2 J). In contrast, the degradation of Om45-HA and Tom22-HA and the steady level of the stable MOM protein Por1 were not affected by deletion of *DOA1* (Fig. S2 K). Therefore, Doa1 itself is specifically required for the turnover of mitochondrial Cdc48 substrates.

Deletion of *DOA1* causes substrate accumulation and mislocalization on mitochondria

The steady levels of Fzo1-HA and Mdm34-HA were significantly elevated in *doa1Δ* cells (Fig. 2 C). We asked where these proteins accumulate in cells. Sub-cellular fractionation experiment showed that Fzo1-HA accumulated in the mitochondria-enriched fraction, but not in the postmitochondria supernatant (PMS), in *doa1Δ* cells (Fig. 2 D). Moreover, when cultured in lactate media (YPL), *doa1Δ* cells had an increased ability to maintain tubular mitochondria in comparison to wild type (WT) cells (Fig. S3 A), indicating that the accumulated Fzo1 is, at least partially, functional.

Mdm34 is an essential component of the ER-mitochondria encounter structure (ERMES) complex that forms punctate foci connecting mitochondria and ER (Kornmann et al., 2009). Similar as Fzo1-HA, Mdm34-HA also accumulated in the mitochondria-enriched fraction in *doa1Δ* and *mdm34$^{\Delta PY}$* cells (Fig. 2 E). We directly monitored the localization of Mdm34 by chromosomal integration of a GFP tag to its C terminus. The fluorescence intensity of the Mdm34-GFP foci was greatly increased in *doa1Δ* and *mdm34$^{\Delta PY}$* cells (Fig. 2, F and G), whereas the number of the Mdm34-GFP foci did not change in the mutant cells (Fig. S3 B). Moreover, we observed diffusive non-punctate signals of Mdm34-GFP on mitochondria in *doa1Δ* and *mdm34$^{\Delta PY}$* cells, but not in WT cells (Fig. 2, F and H), indicating the mislocalization of Mdm34 in the mutant cells. The accumulation of Mdm34 also caused adaptive changes: another two proteins of the ERMES complex, Mmm1 and Mdm12, exhibited increased foci intensities in *doa1Δ* and *mdm34$^{\Delta PY}$* cells (Fig. S3, C–E). These fractionation and imaging results show the accumulation of substrates on mitochondria in *doa1Δ* cells and thus indicate dysfunctions of the Cdc48 complex in extracting and degrading mitochondrial substrates.

The Doa1–Cdc48$^{\cdot Ufd1\text{-}Npl4}$ complex mediates the degradation of mitochondrial Cdc48 substrates

The function of the Cdc48 complex is assisted and diversified by cofactors, including the substrate-recruiting factors (Ufd1-Npl4 heterodimer, Shp1, and Ubx2-7) and substrate-processing factors (Ufd2, Otu1, and Doa1; Stolz et al., 2011; Meyer et al., 2012; Buchberger, 2013). We did a comprehensive analysis of the Cdc48 cofactors and found that only Doa1 and the Ufd1-Npl4 heterodimer are required for the turnover of mitochondrial Cdc48 substrates (Fig. 3, A–C). The Cdc48 cofactor Vms1 was reported to be required for Fzo1 turnover (Heo et al., 2010). However, deletion of *VMS1* did not block Fzo1 degradation, a result consistent with what reported by Esaki and Ogura (Esaki and Ogura, 2012).

Doa1 has a Cdc48-binding PUL domain and two ubiquitin-binding domains (UBDs), WD40 and PFU (Fig. 3 D). The structures of these domains have been resolved individually (Mullally et al., 2006; Fu et al., 2009; Zhao et al., 2009; Nishimasu et al., 2010; Pashkova et al., 2010; Qiu et al., 2010). The recombinant UBDs bind monoubiquitin in vitro (Mullally et al., 2006; Fu et al., 2009; Pashkova et al., 2010), but whether they are required for protein turnover in vivo is unknown. We generated Doa1 mutants by mutating the critical residues in each domain according to previous studies (Fig. 3 D) and replaced the endogenous *DOA1* with the mutants. The expression levels of the Doa1 mutants were comparable to that of WT Doa1 (Fig. 3 E). Mutating the WD40 (WD40$^{\Delta Ub}$) and PUL (PUL$^{\Delta Cdc48}$) domains inhibited the degradation of all the three substrates (Fzo1-HA, Mdm34-HA, and Msp1-HA); mutating the PFU domain (PFU$^{\Delta Ub}$) specifically inhibited the degradation of Msp1-HA, but not the other two substrates (Fig. 3 F). Our results suggest the WD40 UBD is more important than the PFU UBD in substrate turnover, which is consistent with studies showing that the affinity for monoubiquitin of the WD40 domain (K_d ~40 µM) (Pashkova et al., 2010) is substantially higher than that of the PFU domain (K_d ~1 mM; Fu et al., 2009).

The Ufd1–Npl4 heterodimer binds to the N terminus of Cdc48; Doa1 binds to the C terminus of Cdc48 (Stolz et al., 2011; Buchberger, 2013). Immunoprecipitation (IP) of Doa1-FLAG pulled down Cdc48 and Ufd1-HA, confirming the formation of the Doa1–Cdc48$^{\cdot Ufd1\text{-}Npl4}$ complex. As expected, this complex was disrupted by the PUL$^{\Delta Cdc48}$ mutation, but not by the WD40$^{\Delta Ub}$ mutation (Fig. 3 G). Collectively, our results suggest that the Doa1–Cdc48$^{\cdot Ufd1\text{-}Npl4}$ complex mediates the turnover of mitochondrial Cdc48 substrates and that the UBDs of Doa1, especially the WD40 domain, are indispensable for substrate degradation (Fig. 3 H).

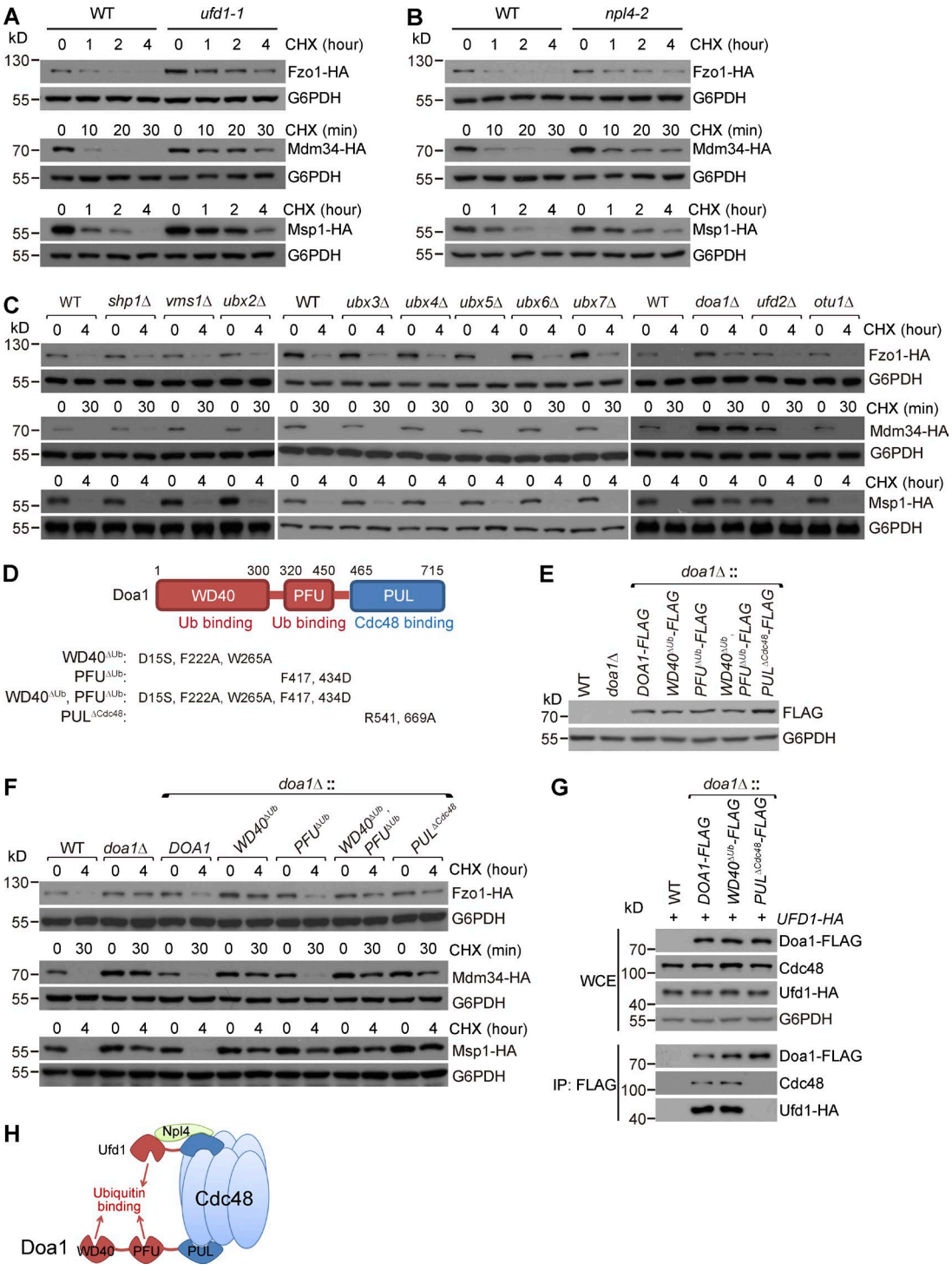

Figure 3. **The Doa1–Cdc48$^{Ufd1\text{-}Npl4}$ complex mediates the degradation of mitochondrial Cdc48 substrates.** (A and B) The *FZO1-HA*, *MDM34-HA*, and *MSP1-HA* strains in WT, *ufd1-1*, or *npl4-2* background were grown to log phase at 25°C and then treated with CHX at 28°C. (C) The *FZO1-HA*, *MDM34-HA*, and *MSP1-HA* strains in WT or the indicated deletion mutant background were grown to log phase and then treated with CHX. (D) Domain architecture of Doa1 and the mutations that disrupt the function of the indicated domains. (E) The coding sequence of *DOA1* was deleted and then replaced with WT or mutated *DOA1* sequences with a C-terminal FLAG tag. Their expression levels were analyzed by anti-FLAG Western blot. (F) The *FZO1-HA*, *MDM34-HA*, and *MSP1-HA* strains in WT or the indicated mutant background were grown to log phase and then treated with CHX. The WD40 and PUL domains of Doa1 were required for the degradation of all the three substrates, whereas the PFU domain was only required for Msp1-HA degradation. (G) The *UFD1-HA* strains in WT, *DOA1-FLAG*, *doa1$^{WD40\Delta Ub}$-FLAG*, or *doa1$^{PUL\Delta Cdc48}$-FLAG* background were subject to anti-FLAG IP. WCE and immunoprecipitates were analyzed by Western blot. (H) Illustration of the Doa1–Cdc48$^{Ufd1\text{-}Npl4}$ complex. Doa1 and the Ufd1-Npl4 heterodimer bind to the C and N terminus of the Cdc48 hexamer, respectively.

Ubiquitinated Fzo1-HA and Mdm34-HA accumulate in the mitochondria-enriched fraction in *doa1Δ* cells

The aforementioned results suggest that Doa1 is a key Cdc48 cofactor mediating the turnover of mitochondrial substrates. The Cdc48 complex interacts with ubiquitinated substrates and extracts them from organelle membranes. Ubiquitinated substrates accumulate in cells upon the inactivation of Cdc48 (Stolz et al., 2011; Meyer et al., 2012; Buchberger, 2013). If Doa1 is required for the removal of ubiquitinated mitochondrial substrates, accumulation of ubiquitinated substrates in *doa1Δ* cells would be expected.

We could not detect substrate ubiquitination by Western blot analysis of whole-cell extracts (WCEs; unpublished data), indicating that the ubiquitinated species are present in low amounts. We therefore performed IP of substrates. In WT cells, we observed up-shifted bands of Fzo1-HA, which were greatly increased in *cdc48-3* cells (Fig. 4 A, lane 1 vs. 2). Deletion of *MDM30*, the ubiquitin E3 ligase of Fzo1 (Cohen et al., 2008), abolished the formation of Fzo1-HA upshifts in WT and *cdc48-3* cells (Fig. 4 B, lane 2 vs. 3 and lane 4 vs. 5), indicating that the upshifts are very likely to be the ubiquitinated forms of Fzo1-HA (Ub-Fzo1-HA). Accumulation of such upshifts was also seen in *doa1Δ* cells (Fig. 4 A, lane 3). By overexpressing and probing 3xFLAG-tagged ubiquitin, we confirmed that the upshifts of Fzo1-HA in *doa1Δ* cells are indeed Ub-Fzo1-HA (Fig. 4 C). We rescued ubiquitin level in *doa1Δ* cells, which actually further enhanced the accumulation of Ub-Fzo1-HA (Fig. 4 A, lane 5 vs. 6), indicating that the accumulation of Ub-Fzo1-HA in *doa1Δ* cells is not caused by ubiquitin depletion. We then performed IP of Fzo1-HA from different subcellular fractions and found that Ub-Fzo1-HA was only present in the mitochondria-enriched, but not the PMS, fraction of *cdc48-3* and *doa1Δ* cells (Fig. 4 D).

Upshifts of HA signals indicate Ub-Fzo1-HA (Fig. 4, A–C), but we could not see similar upshifts of Mdm34-HA, indicating Ub-Mdm34-HA is present in very low amounts. Therefore, we overexpressed FLAG-ubiquitin using a 2μ plasmid, and after IP of Mdm34-HA, we probed the immunoprecipitates with anti-FLAG antibody to detect Ub-Mdm34-HA. In this way, we observed that Ub-Mdm34-HA accumulated in *cdc48-3* and *doa1Δ* cells (Fig. 4 E, lane 2 vs. 3 and 4). Mutating Rsp5, the E3 ligase of Mdm34, or the PY motif of Mdm34 ($Mdm34^{\Delta PY}$) increased the protein level of Mdm34-HA, but greatly reduced its ubiquitination (Fig. 4 E, lane 2 vs. 5 and 6). Same as Ub-Fzo1-HA, Ub-Mdm34-HA was only present in the mitochondria-enriched fraction of *cdc48-3* and *doa1Δ* cells (Fig. 4 F, lanes 2–4 vs. 6–8). These results suggest that Doa1 and Cdc48 are required to extract ubiquitinated MAD substrates from mitochondria.

Doa1 facilitates the recruitment of ubiquitinated Fzo1-HA and Mdm34-HA to the $Cdc48^{Ufd1\text{-}Npl4}$ complex

Doa1 may function in two processes on the Cdc48 complex: recruiting ubiquitinated substrates to Cdc48 or transferring the unfolded substrates from Cdc48 to downstream ubiquitin receptors. Deletion of *DOA1* will reduce the amount of Cdc48-associated substrates if it mediates substrate recruitment to Cdc48, or deletion of *DOA1* will increase the amount of Cdc48-associtated substrates if it mediates the release of substrates from Cdc48.

It is reported that Cdc48 inactivation in *cdc48-3* cells prevents substrate extraction and stabilizes the interaction between the Cdc48 complex and ubiquitinated substrates (Verma et al., 2011; Nakatsukasa et al., 2013). Consistently, IP of Fzo1-HA showed that both Fzo1 ubiquitination and its interaction with Cdc48 were very weak in WT cells (Fig. 5 A, lane 2) but were greatly increased in *cdc48-3* cells (Fig. 5 A, lane 4). Fzo1 ubiquitination was also increased in *doa1Δ* cells; however, its interaction with Cdc48 was not increased as seen in *cdc48-3* cells (Fig. 5 A, lane 2 vs. 3), indicating Doa1 is unlikely to mediate substrate-releasing from Cdc48. Furthermore, when we deleted *DOA1* in *cdc48-3* cells, Fzo1-HA ubiquitination was not affected, but its interaction with Cdc48 was significantly reduced (Fig. 5 A, lane 4 vs. 5). Similarly, IP of Mdm34-HA also showed a significant increase in the interaction of Cdc48 and Mdm34-HA in *cdc48-3* cells, and the interaction was disrupted by deleting *DOA1* (Fig. 5 B, lane 4 vs. 5). These results suggest that Doa1 facilitates substrate recruitment to Cdc48.

To further investigate the interaction between Fzo1-HA and the $Cdc48^{Ufd1\text{-}Npl4}$ complex, we analyzed the Ufd1- and Cdc48-associated Fzo1-HA. In the Ufd1-Npl4 heterodimer, Ufd1 is the one that directly interacts with ubiquitinated substrates (Stolz et al., 2011; Buchberger, 2013). IP of Ufd1-FLAG and FLAG-Cdc48 showed that Ufd1 and Cdc48 associated with a small amount of nonubiquitinated Fzo1-HA and Ub-Fzo1-HA in WT cells, and the interactions were significantly increased in *cdc48-3* cells (Fig. 5, C and D). The nonubiquitinated Fzo1-HA pulled down by Ufd1-FLAG and FLAG-Cdc48 is real because we did not pull down Fzo1-HA from cells lacking FLAG-tagged baits (Fig. 5, C and D, first lanes). The nonubiquitinated Fzo1-HA could be indirectly pulled down because of the oligomeric nature of the Fzo1 complex (Rapaport et al., 1998; Griffin and Chan, 2006; Anton et al., 2011). Indirect association of Cdc48 with nonubiquitinated substrates has already been observed for other Cdc48 substrates (Shcherbik and Haines, 2007).

Consistent with the Fzo1-HA IP results (Fig. 5 A), deletion of *DOA1* significantly reduced the amount of the Ufd1- and Cdc48-associated nonubiquitinated Fzo1-HA and Ub-Fzo1-HA in *cdc48-3* cells (Fig. 5, E [lane 4 vs. 5] and F [lane 4 vs. 5]). In Fig. 5 F, ubiquitin level was restored by ubiquitin overexpression to avoid possible side effects caused by ubiquitin depletion in *doa1Δ* cells. Collectively, these results strongly suggest that Doa1 is required for the efficient recruitment of mitochondrial substrates to the $Cdc48^{Ufd1\text{-}Npl4}$ complex.

The Ufd1–Npl4 heterodimer serves as a substrate-recruiting complex in other Cdc48-mediated degradation pathways (Stolz et al., 2011; Buchberger, 2013). To examine its function in MAD, we introduced *npl4-2*, a conditional mutant allele of Npl4, to *cdc48-3* cells. Inactivation of the Ufd1-Npl4 heterodimer enhanced the accumulation of Ub-Fzo1-HA (Fig. 5 G, lane 2 vs. 3) but greatly reduced the interaction between Cdc48 and Ub-Fzo1-HA (Fig. 5 H, lane 2 vs. 3). Thus, the Ufd1-Npl4 heterodimer is also required for the recruitment of MAD substrates to Cdc48. Given that Doa1 is required for the recruitment of Ub-Fzo1-HA to Ufd1 (Fig. 5 E), the Ufd1–Npl4 complex may function downstream of Doa1 in the substrate-recruitment process.

Doa1 interacts with ubiquitinated Fzo1-HA

The Ufd1-Npl4 heterodimer is required for the turnover of most Cdc48 substrates. But in many cases, the $Cdc48^{Ufd1\text{-}Npl4}$ complex alone is not enough for substrate degradation, and additional UBX family substrate-recruiting factors are required (Baek et al., 2013; Buchberger, 2013). For example, Ubx2 and Ubx5 link the $Cdc48^{Ufd1\text{-}Npl4}$ complex to ER (Neuber et al.,

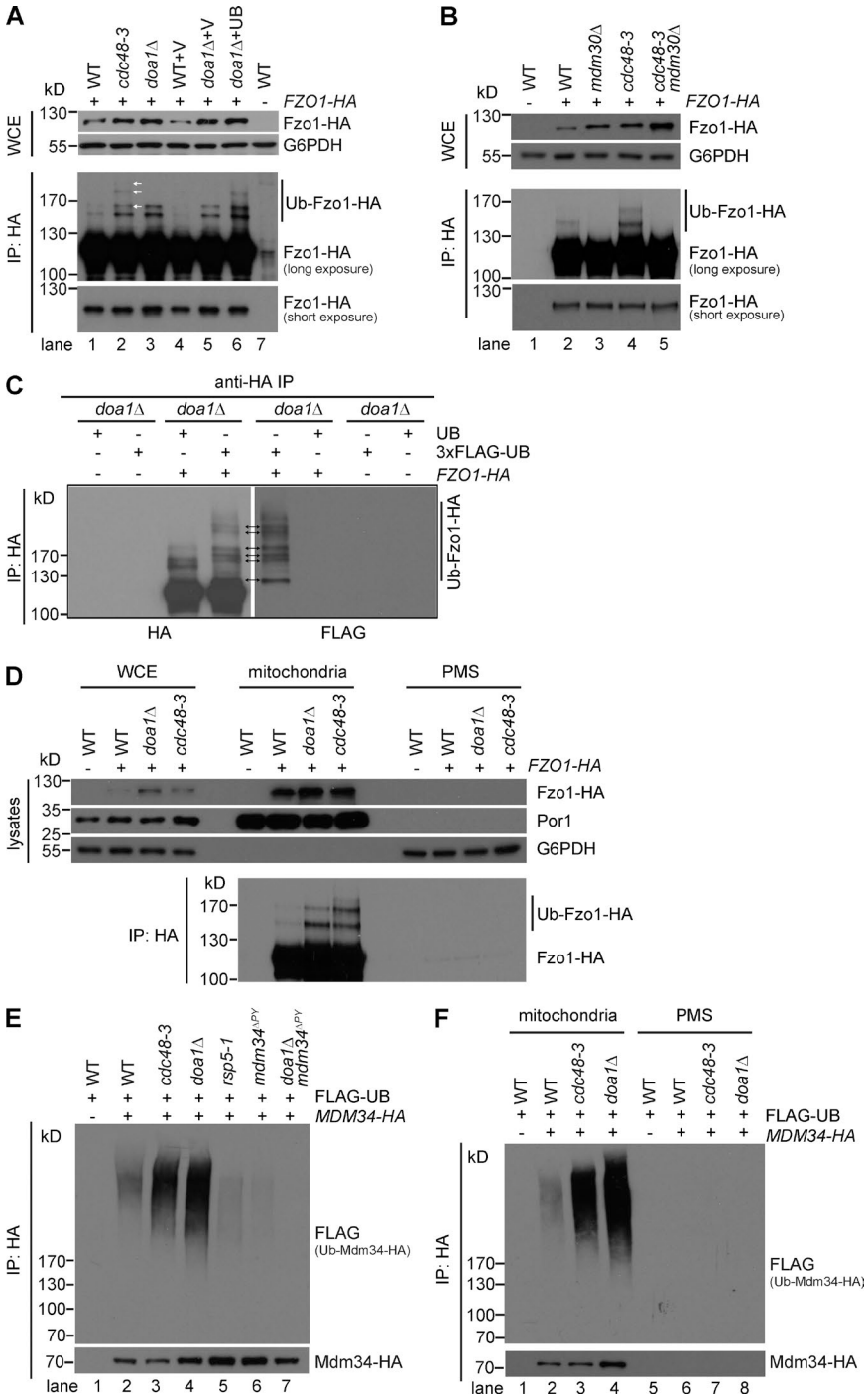

Figure 4. **Deletion of *DOA1* causes the accumulation of ubiquitinated Fzo1-HA and Mdm34-HA in the mitochondria-enriched fraction.** (A and B) The *FZO1-HA* strains in WT or the indicated mutant background were grown to log phase at 28°C before being subject to anti-HA IP. WCE and immunoprecipitates were analyzed by Western blot. The anti-HA antibody was used to probe the nonubiquitinated and ubiquitinated Fzo1-HA (Ub-Fzo1-HA). (C) The *doa1Δ* and *FZO1-HA doa1Δ* strains were transformed with high-copy ubiquitin-expressing plasmids (UB or 3xFLAG-UB as indicated). The anti-HA immunoprecipitates were analyzed by anti-HA and anti-FLAG antibodies. In comparison with cells transformed with UB, cells harboring 3xFLAG-UB slowed the migration of Ub-Fzo1-HA. The corresponding bands on both blots are highlighted by arrows. (D) Lysates from the mitochondria-enriched and PMS fractions of the indicated strains (grown at 28°C) were subject to anti-HA IP. Lysates from different fractions and immunoprecipitates were analyzed by Western blot. (E) The *MDM34-HA* strains in WT or the indicated mutant background were transformed with a high-copy ubiquitin-expressing plasmid (FLAG-UB) and grown to log phase at 28°C. The anti-HA immunoprecipitates were analyzed by anti-HA and anti-FLAG antibodies. Ub-Mdm34-HA: ubiquitinated Mdm34-HA. (F) Lysates from the mitochondria-enriched and PMS fractions of the indicated strains (grown at 28°C) were subject to anti-HA IP. The immunoprecipitates were analyzed as in E.

2005; Schuberth and Buchberger, 2005) and nuclear (Verma et al., 2011) substrates, respectively. If Doa1 plays a similar role in MAD as the UBX proteins, Doa1 may interact with ubiquitinated MAD substrates through its UBDs, which are essential for substrate degradation (Fig. 3 F).

IP of Doa1-FLAG showed that Doa1-FLAG interacted weakly with nonubiquitinated Fzo1-HA and Ub-Fzo1-HA in WT cells. The interaction, especially with Ub-Fzo1-HA, was greatly enhanced in *cdc48-3* cells (Fig. 6 A, lane 2 vs lane 3). The Doa1-associated Ub-Fzo1-HA resembles the major forms of Ub-Fzo1-HA accumulated in *cdc48-3* cells (the three Ub-Fzo1-HA bands in Fig. 4 A, lane 2, white arrows), and has a distinct pattern from the Ufd1- and Cdc48-associated Ub-Fzo1-HA (compare Fig. 6 A, lane 3, with Fig. 5, C [lane 3] and D [lane 3]). Therefore, it is unlikely that Doa1 indirectly interacts with substrates through its association with the Cdc48$^{Ufd1\text{-}Npl4}$ complex.

Deletion of *MDM30*, the E3 ligase of Fzo1 (Cohen et al., 2008), abolished the interaction of Doa1-FLAG with nonubiquitinated Fzo1-HA and Ub-Fzo1-HA in WT (Fig. 6 B, lane 2 vs. 3) and *cdc48-3* (Fig. 6 B, lane 4 vs. 5) cells. These results suggest the Doa1-associated nonubiquitinated Fzo1-HA is indirectly pulled down because of the oligomeric nature of Fzo1.

The WD40 UBD of Doa1 is required for Fzo1 turnover (Fig. 3 F). Consistently, mutating the WD40 domain greatly inhibited the interaction between Doa1-FLAG and Fzo1-HA (Fig. 6 C, lane 2 vs. 3). However, the truncated Doa1 containing

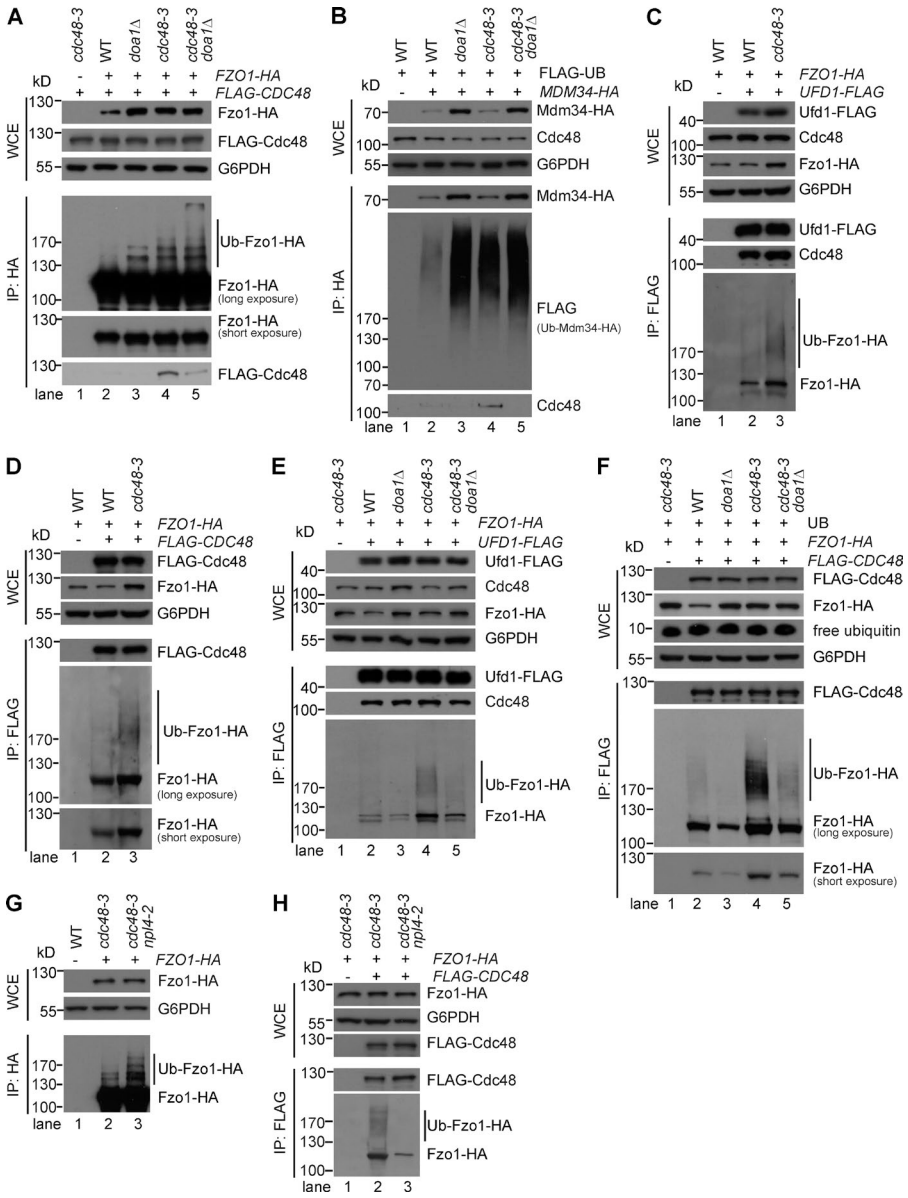

Figure 5. **Doa1 is required for the recruitment of ubiquitinated Fzo1-HA and Mdm34-HA to the Cdc48$^{Ufd1\text{-}Npl4}$ complex.** (A–H) The indicated strains were grown to log phase at 28°C before being subject to anti-HA (A, B, and G) or anti-FLAG (C–F and H) IP. WCE and immunoprecipitates were analyzed by Western blot. Strains in B and F were transformed with a high-copy plasmid expressing FLAG-ubiquitin (FLAG-UB) and ubiquitin (UB), respectively.

the two UBDs (WD40 + PFU) was not able to pull down Fzo1-HA (Fig. 6 D, lane 2 vs. 5), indicating UBDs are not sufficient for substrate-binding in vivo. Similarly, the WD40 domain alone could not interact with Fzo1-HA (Fig. 6 D, lane 2 vs. 4). We further tested the PUL$^{\Delta Cdc48}$ mutant, which disrupts the interaction with Cdc48 but largely preserves the PUL domain. In comparison with the Doa1 fragment containing the UBDs, the PUL$^{\Delta Cdc48}$ mutant had a slightly stronger interaction with Fzo1-HA (Fig. 6 D, lane 3 vs. 5). But the interaction was still much weaker than the binding between WT Doa1 and Fzo1-HA (Fig. 6, C [lane 2 vs. 4] and D [lane 2 vs. 3]), indicating that interaction with Cdc48 is required for Doa1 to bind its physiological ubiquitinated substrates.

Doa1 accumulates on mitochondria in *cdc48-3* cells

The aforementioned characterizations showed that the interaction between mitochondrial substrates and the Doa1–Cdc48$^{Ufd1\text{-}Npl4}$ complex is stabilized in *cdc48-3* cells. The interaction may be stabilized on mitochondria, because inactivation of Cdc48 prevents the retrotranslocation of ubiquitinated substrates from membranes (Verma et al., 2011; Nakatsukasa et al., 2013). We did subcellular fractionation experiments and detected a significantly increased amount of ubiquitinated proteins and Doa1-FLAG in the mitochondrial-enriched fraction in *cdc48-3* cells as compared with WT cells (Fig. 6 E, lane 3 vs. 4). We further showed that Doa1 peripherally associates with MOM because it was completely degraded by Proteinase K added to intact mitochondria (Fig. S4 A) and was extracted from mitochondria by sodium carbonate (Fig. S4 B).

The amount of Ufd1-FLAG in the mitochondrial-enriched fraction was also increased in *cdc48-3* cells (Fig. S4 C, lane 3 vs. lane 4), but to a much lesser extent in comparison with Doa1-FLAG. The underlying reason for such a difference could be that a Cdc48 hexamer can only bind one pair of Ufd1-Npl4 heterodimer (Hetzer et al., 2001; Pye et al., 2007), whereas the docking of Doa1 to a Cdc48 hexamer may not have such constraints.

We further analyzed the localization of Doa1 in *cdc48-3* cells by imaging. We fused a GFP tag to the C terminus of Doa1, which did not interfere with Doa1 function (Fig. S4 D).

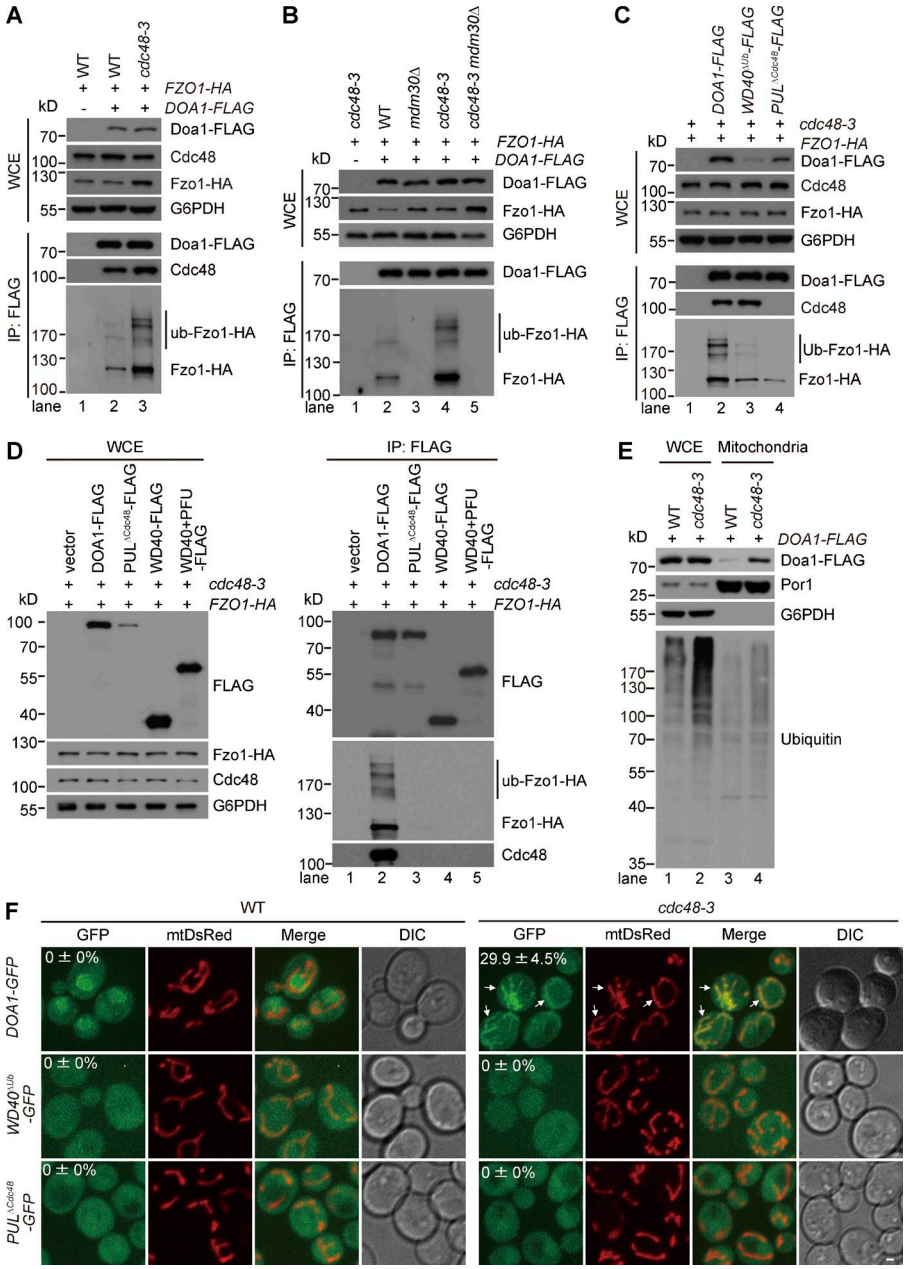

Figure 6. **Doa1 interacts with Ub-Fzol-HA and accumulates on mitochondria in *cdc48-3* cells.** (A–C) The indicated strains were grown to log phase at 28°C before being subject to anti-FLAG IP. WCE and immunoprecipitates were analyzed by Western blot. (D) The *FZO1-HA cdc48-3* strain was transformed with low-copy plasmids expressing FLAG-tagged, WT, or mutant forms of Doa1 and analyzed as in A. (E) Lysates from the WCE and the mitochondria-enriched fraction of the indicated strains (grown at 28°C) were analyzed by Western blot. (F) The *DOA1-GFP*, *doa1*$^{WD40\Delta Ub}$*-GFP*, and *doa1*$^{PUL\Delta Cdc48}$*-GFP* strains in WT or *cdc48-3* background were grown to log phase at 25°C, then switched to 28°C for 5 h before imaging. All the strains chromosomally expressed mtDsRed. Z projections and differential interference contrast images are shown. Bar, 1 µm. White arrows point to cells with mitochondrial localization of Doa1-GFP. The percentages of cells with mitochondrial signals of Doa1-GFP were shown on the top of the GFP images. Data values represent means ± SEM from three independent experiments, with at least 600 cells counted in each experiment.

Doa1-GFP was diffusively distributed in the nucleus and the cytoplasm in WT cells, but was enriched on mitochondria in *cdc48-3* cells (Fig. 6 F). Mutating the WD40 and PUL domains, which were required for substrate interaction (Fig. 6, C and D), inhibited the mitochondrial enrichment of Doa1-GFP (Fig. 6 F).

Doa1 is not essential for surviving ER stress

Previous studies demonstrate that the Ubx2–Cdc48$^{Ufd1\text{-}Npl4}$ complex mediates ERAD (Ye et al., 2001; Jarosch et al., 2002; Neuber et al., 2005; Schuberth and Buchberger, 2005). Our study suggests that MAD and ERAD share the core Cdc48$^{Ufd1\text{-}Npl4}$ complex but have different additional Cdc48 cofactors: MAD requires Doa1, and ERAD requires the ER-resident Ubx2 (Fig. 7 A). To determine whether Doa1 is an ERAD component, we performed the following growth tests.

The lack of ERAD components strongly compromises the viability of cells that cannot elicit unfolded protein response (UPR) at 37°C (Friedlander et al., 2000; Ng et al., 2000). Accordingly, cells lacking *UBX2* or *IRE1*, a key UPR component (Cox et al., 1993), grew normally, but cells lacking both genes showed severe growth defects at 37°C (Fig. 7 B). Similarly, double knockout of *IRE1* and *HRD1*, another key ERAD component (Hampton et al., 1996), caused strong synthetic growth defects at 37°C as shown previously (Friedlander et al., 2000; Fig. 7 C). In contrast, deletion of *DOA1* in *ire1Δ* cells did not affect cell growth (Fig. 7, B and C). Therefore, Doa1 is unlikely an essential ERAD component. Our result is consistent with the previous study that *doa1Δ* cells were insensitive to the treatment of the ERAD inducer tunicamycin (Mullally et al., 2006).

We further examined the role of Doa1 in the degradation of an ERAD-lumen substrate, CPY* (Hiller et al., 1996), and an ERAD-cytoplasm substrate, Ubc6 (Swanson et al., 2001; Walter et al., 2001). CPY*-FLAG degradation was inhibited in *ubx2Δ* and *doa1Δ* cells, but the degradation defect in *doa1Δ* cells was rescued by ubiquitin overexpression (Fig. S5 A). The

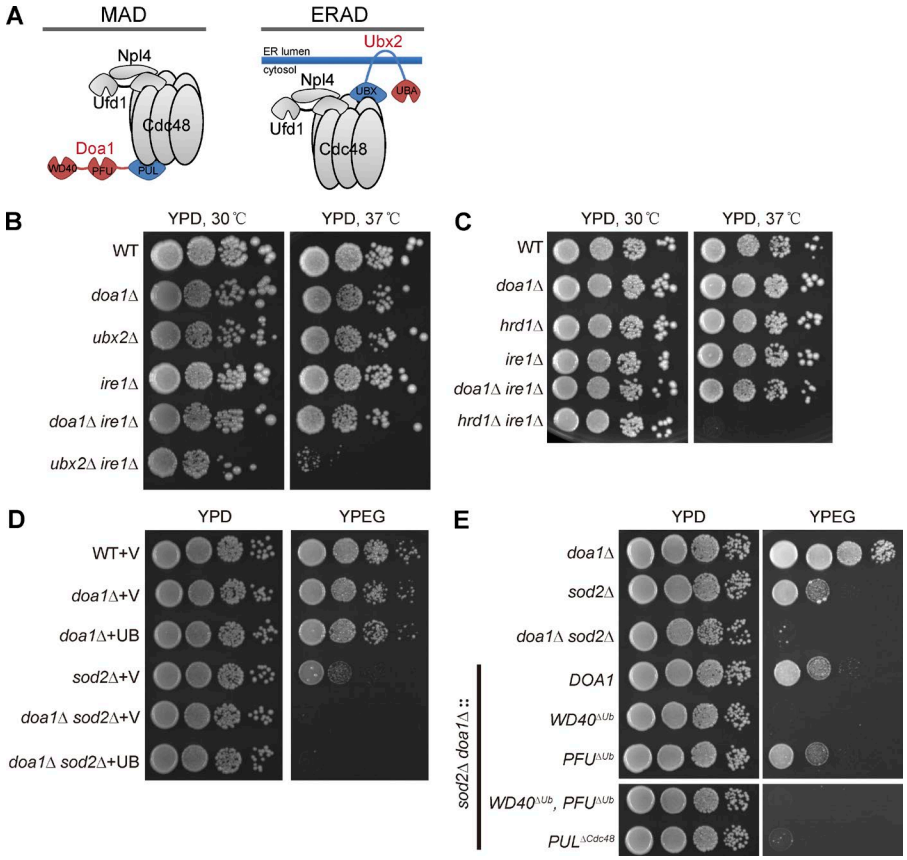

Figure 7. **Doa1 is critical for cell survival under mitochondrial oxidative stress, but not ER stress, conditions.** (A) Illustration of the Cdc48 complexes for MAD and ERAD, respectively. (B) The indicated strains in W303 strain background were grown in glucose media to log phase and then spotted on glucose (YPD) plates in a 10-fold serial dilution and then incubated for 3 d at 30°C or 37°C. (C) The indicated strains in BY4741 strain background were analyzed as in B. (D) The indicated strains were grown in glucose media to log phase and then spotted on YPD or ethanol and glycerol (YPEG) plates in a 10-fold serial dilution, and then incubated for 2–4 d at 30°C. (E) The indicated strains were analyzed as in D. WT or mutated *DOA1* sequences were integrated into the chromosomal locus of *DOA1* in *sod2Δ doa1Δ* cells. The growth test result of the last two strains was cut out from the full image shown in Fig. S5 H.

degradation of Ubc6-HA was inhibited by inactivation of Ufd1 but was normal in *doa1Δ* cells (Fig. S5 B). Deletion of *DOA1* did not affect the degradation of a cytoplasmic Cdc48 substrate (prematurely terminated Gnd1^{PTC}) either (Verma et al., 2013; Fig. S5 C). These results suggest that Doa1 does not directly mediate the turnover of these nonmitochondrial Cdc48 substrates. Although deletion of *DOA1* may indirectly affect the turnover of some ERAD substrates because of ubiquitin depletion, it does not cause global impairment of ERAD as suggested by the growth tests.

Doa1 is required for surviving mitochondrial oxidative stress

The *doa1Δ* cells had no overt growth defect under normal conditions. We therefore proceeded to investigate whether deletion of *DOA1* affects cell survival under mitochondrial stress conditions. We analyzed the synthetic growth phenotype between *doa1Δ* and the deletion of other mitochondrial quality-control genes, including *SOD2*, a matrix superoxide scavenger (van Loon et al., 1986); mitochondrial AAA proteases, including *YME1*, *YTA12*, *AFG3*, and *PIM1* (Quirós et al., 2015); and *ATG32*, a mitophagy receptor (Kanki et al., 2009; Okamoto et al., 2009). Deletion of *DOA1* did not affect the growth of *atg32Δ* (Fig. S5 D) or *yme1Δ* cells (Fig. S5 E), but it mildly inhibited the growth of *yta12Δ* and *afg3Δ* cells (Fig. S5 F) and strongly inhibited the growth of *pim1Δ* cells (Fig. S5 G). Besides the degradation of damaged mitochondrial proteins, Yta12 and Afg3 are required for the assembly of inner membrane complexes (Arlt et al., 1996), and Pim1 is required for the maintenance of mtDNA (Suzuki et al., 1994; Van Dyck et al., 1994). Therefore, the synthetic growth defects of *doa1Δ* and the deletion of mitochondrial proteases may be caused by compound effects.

In comparison to WT cells, deletion of *SOD2*, which elevates mitochondrial oxidative stress, compromised cell growth in ethanol and glycerol (YPEG) media (Fig. 7 D). YPEG media are nonfermentable and thus require mitochondrial respiration for cell growth. This growth defect was further exacerbated upon the deletion of *DOA1* and could not be rescued by ubiquitin overexpression (Fig. 7 D). The synthetic growth defect of *doa1Δ sod2Δ* cells was rescued by *doa1*$^{PFU\Delta Ub}$, but not by *doa1*$^{WD40\Delta Ub}$, *doa1*$^{WD40\Delta Ub,\ PFU\Delta Ub}$, or *doa1*$^{PUL\Delta Cdc48}$ mutants (Fig. 7 E), further supporting that the WD40 and PUL domains are essential for Doa1 function. These results suggest Doa1 is critical for surviving mitochondrial oxidative stress.

Discussion

MAD is an integral part of the mitochondrial quality control system. We analyzed the turnover of a subset of MOM proteins and identified Cdc48 substrates (Fig. 1) and potential Cdc48-independent substrates (Fig. S1). This observation, as well as a recent discovery that another AAA ATPase Msp1 mediates the degradation of mistargeted proteins on MOM (Chen et al., 2014; Okreglak and Walter, 2014), suggests MAD is more complex than expected.

Using the newly identified mitochondrial Cdc48 substrate Tom70, we established a genetic screen assay to unbiasedly characterize the genetic basis of the Cdc48-dependent MAD pathway. Our pilot screen identified several regulators, including the Cdc48 cofactor Doa1 and the ubiquitin E3 ligase Rsp5 (Fig. S2). Although the characterization of the Cdc48-dependent MAD pathway is at its beginning, our study has made several interesting observations.

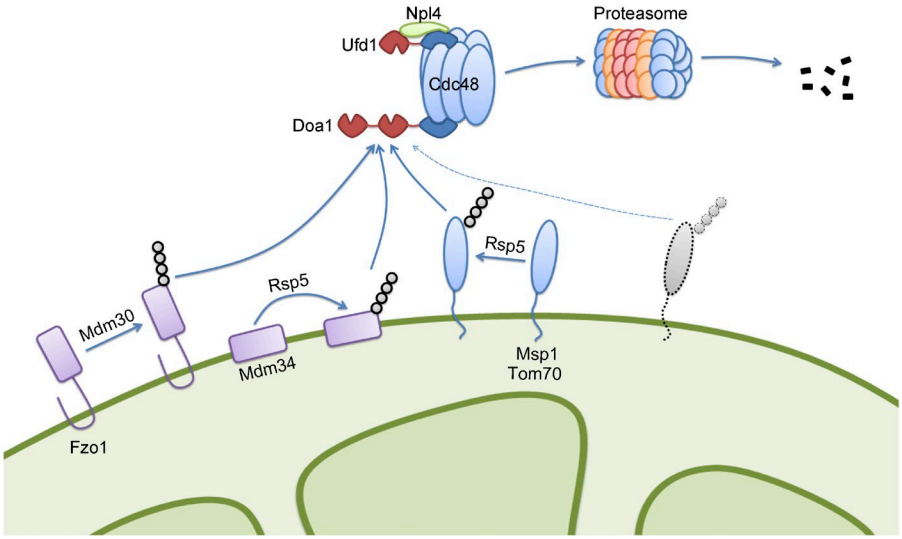

Figure 8. **Cartoon illustration of the MAD pathway mediated by the Doa1–Cdc48$^{Ufd1\text{-}Npl4}$ complex.** MOM proteins with different topologies are ubiquitinated by ubiquitin E3 ligases, such as Mdm30 and Rsp5. Doa1 in the Doa1-Cdc48$^{Ufd1\text{-}Npl4}$ complex is the primary factor to recognize and recruit ubiquitinated MOM proteins to the Ufd1–Npl4 heterodimer and then to Cdc48. By hydrolyzing ATP, Cdc48 dislodges ubiquitinated MOM proteins from membrane and presents them to proteasome for degradation. The dashed lines indicate potential additional mitochondrial substrates of Doa1.

We provide genetic and biochemical evidence that the Doa1–Cdc48$^{Ufd1\text{-}Npl4}$ complex mediates the turnover of mitochondrial Cdc48 substrates (Fig. 8). The degradation of Cdc48 substrates is mostly mediated by the core Cdc48$^{Ufd1\text{-}Npl4}$ complex and often assisted by additional substrate-recruiting factors, including Ubx2-7 (Stolz et al., 2011; Meyer et al., 2012; Baek et al., 2013; Buchberger, 2013). In the absence of these additional substrate-recruiting factors, substrate recruitment to the Cdc48$^{Ufd1\text{-}Npl4}$ complex and the subsequent substrate degradation are partially or completely inhibited (Schuberth and Buchberger, 2005; Alexandru et al., 2008). MAD shares the same core Cdc48$^{Ufd1\text{-}Npl4}$ complex with other Cdc48-dependent degradation pathways, and utilizes Doa1 to interact with the ubiquitinated substrate Fzo1 (Fig. 6) and facilitate substrate recruitment to the Cdc48$^{Ufd1\text{-}Npl4}$ complex (Fig. 5). Although the biochemical studies were focused on Fzo1 and Mdm34, Doa1 may regulate the degradation of other mitochondrial substrates in a similar manner. We thus propose that Doa1 functions as a substrate-recruiting factor of Cdc48 in MAD. A notable difference between Doa1 and the other substrate-recruiting factors is that Doa1 binds to the C terminus, whereas the others bind to the N terminus of Cdc48. Our observation highlights the complexity and flexibility of substrate handling on the Cdc48 complex.

Doa1 antagonizes the degradation of the Ufd2-dependent substrates, including the UFD pathway substrate Ubi-Pro–β-galactosidase and the OLE pathway substrate Spt23 (Rumpf and Jentsch, 2006). In contrast to these substrates, the degradation of mitochondrial Cdc48 substrates is Ufd2 independent but Doa1 dependent (Fig. 3). Thus, our results and previous characterizations highlight Doa1 as a unique factor playing dual roles in the degradation of Cdc48 substrates: for Ufd2-dependent substrates, it is a substrate-processing factor inhibiting degradation; for Ufd2-independent mitochondrial Cdc48 substrates, it is a substrate-recruiting factor promoting degradation.

Doa1 has an interesting property that only the Cdc48-bound Doa1 can interact with substrates, whereas the Cdc48-unbound Doa1 or its UBDs alone cannot (Fig. 6, C and D), which brings a potential benefit that the Cdc48-unbound Doa1 does not bind substrates to interfere with substrate degradation. The underlying molecular mechanism is not clear, but it is conceivable that conformational changes may occur when Doa1 interacts with Cdc48, which has been suggested by structural studies of the PUL domain (Zhao et al., 2009; Nishimasu et al., 2010) and has been observed for other Cdc48 cofactors (Beuron et al., 2006; Bebeacua et al., 2012).

An intriguing observation is that in *cdc48-3* cells, in which Cdc48 substrates accumulate at many subcellular locations, Doa1 selectively enriches on mitochondria (Fig. 6 F). This observation indicates that a significant portion of, if not all, Doa1 substrates is mitochondrial. Considering that our analysis of MOM proteins (14 experimentally verified transmembrane proteins) only covers a small percentage of the MOM proteome (>110 proteins predicted by mass spectrometry analysis; Zahedi et al., 2006), we speculate that Doa1 may have more mitochondrial substrates not identified yet. It is unclear whether the recognition of mitochondrial Cdc48 substrates by Doa1 involves specific molecular mechanisms. A genome-wide genetic screen and further biochemical characterizations are thus necessary for a better understanding of the Cdc48-dependent MAD pathway.

Doa1 is highly conserved during evolution. Structural studies and sequence analyses show that the domain organization and the critical residues are highly conserved between Doa1 and its mammalian orthologue PLAA (Mullally et al., 2006; Fu et al., 2009; Pashkova et al., 2010; Qiu et al., 2010). It will be interesting to examine if PLAA is also involved in the mammalian MAD pathway in the future.

Materials and methods

Yeast strains and media

The yeast strains used in this study are listed in Table S3. Strain transformation was performed using standard protocols (Longtine et al., 1998; Voth et al., 2001; Janke et al., 2004). Yeast strains were grown at 30°C if not otherwise indicated. BY4741, W303-1A, and CEN.PK strains were gifts from B. Tu (University of Texas Southwestern, Dallas, TX).

Media used in this study (Sherman, 2002) included YPD (1% yeast extract, 2% peptone, and 2% glucose), YPL (1% yeast extract, 2% peptone, and 2% lactate), YPEG (1% yeast extract, 2% peptone, 3% ethanol, and 3% glycerol), YPGAL (1% yeast extract, 2% peptone, and 2% galactose), SCD (0.67% yeast nitrogen base without amino acids, 0.079% complete supplement mixture, and 2% glucose), SCEG (0.67% yeast nitrogen base without amino acids, 0.079% complete supplement mixture, 3% ethanol, and 3% glycerol), SCD-LEU (0.67% yeast

nitrogen base without amino acids, 0.069% -Leu DO supplement, and 2% glucose), SCD-URA (0.67% yeast nitrogen base without amino acids, 0.077% -Ura DO supplement, and 2% glucose), and SCGAL-URA (0.67% yeast nitrogen base without amino acids, 0.077% -Ura DO supplement, and 2% galactose). ClonNAT (100 µg/l; WERNER BioAgents) was added to media for plasmid maintenance as needed.

Antibodies and chemicals

The following antibodies were from Sigma-Aldrich: glucose-6-phosphate dehydrogenase (G6PDH), HA-peroxidase, and FLAG M2. Antibodies for ubiquitin (P4D1) and VCP/Cdc48 were from Cell Signaling Technology. The antibody for Por1 was from Thermo Fisher Scientific. The GFP antibody was obtained from CWbio.

Yeast extract, peptone, and yeast nitrogen base without amino acids were purchased from BD. Yeast complete supplement mixture was purchased from MP Biomedicals. Yeast amino acid dropout supplements were obtained from Takara Bio Inc. CHX was obtained from Amresco. MG132 was from EMD Millipore. Other chemicals or reagents were obtained from Sigma-Aldrich if not otherwise indicated.

Yeast plasmids

Plasmids used in this study are listed in Table S4.

The ubiquitin expression plasmids pRS42N-UB, pRS42N-3xFLAG-UB, pRS425-UB, and pRS425-1xFLAG-UB were generated as follows: the ubiquitin coding sequence (with or without a 1xFLAG right after the start codon) was first inserted into p417-TEF1 (Wu and Tu, 2011) at the BamHI–EcoRI sites; a 3xFLAG tag was inserted into the resulting plasmid at SpeI–BamHI sites; the ubiquitin coding sequence with or without the 1x or 3xFLAG tag, together with the promoter and terminator sequences, were then excised at the ApaI–NotI sites and inserted into pRS42N or pRS425 (Christianson et al., 1992; Taxis and Knop, 2006).

The plasmids expressing full-length or truncated forms of *DOA1* were generated as follows: the TEF1 promoter in p417-TEF1-natNT2 (KanMX4 in p417-TEF1 was replaced by natNT2) was replaced with the GAL1 promoter at SacI–XbaI sites; a 3xFLAG tag was inserted into the resulting plasmid at EcoRI–SalI sites; the full-length coding sequence of *DOA1*, the WD40 domain (1–900 bp of *DOA1*), and the WD40+PFU domain (1–1350 bp of *DOA1*) were then inserted into the plasmid (natNT2-GAL1-3XFLAG-C) from the last step at XbaI–SpeI sites to make plasmids natNT2-GAL1-DOA1-FLAG, natNT2-GAL1-WD40-FLAG, and natNT2-GAL1-WD40+PFU-FLAG. Point mutations R541A and R669A in the PUL domain were created by QuikChange site-directed mutagenesis (Agilent Technologies).

The pYES2-CPY^{G255R} (CPY*)-FLAG plasmid was created as follows: the coding sequence for 3xFLAG was inserted into pYES2 (Thermo Fisher Scientific) at the BamHI–EcoRI sites, the *CPY* coding sequence was then inserted into the resulting plasmid at the HindIII–KpnI sites, and the G255R mutation was introduced by QuikChange site-directed mutagenesis.

The hphNT1-TEF1-UBC6-HA plasmid was generated as follows: a 1xHA tag was inserted in between Leu^{201} and Asp^{202} of Ubc6 by isothermal assembly (Gibson et al., 2009), and then the full-length coding sequence of *UBC6* with the internal 1xHA tag was inserted to p417-TEF1-hphNT1 (KanMX4 in p417-TEF1 was replaced by hphNT1) at BamHI–SalI sites.

Plasmids pRS42N, pRS425, p417-TEF1, and pYES2 were gifts from B. Tu.

Colony screen assay

To randomly generate insertion mutants by homologous recombination (Burns et al., 1994), the founder strain *TOM70-HA, leu2Δ* was transformed with the yeast genomic mini-Tn3::lacZ::LEU2 transposon insertion library (provided by B. Tu). Approximately 5,000 mutants were generated and tested by colony assay. On day 0, the transformed yeast cells were grown on selective glucose (SCD-LEU) plates. On day 3, we replica-plated the cells from the SCD-LEU plates to lactate (YPL) plates. On day 4, these cells were replica-plated onto nitrocellulose membranes that were placed on YPL plates. On day 5, the nitrocellulose membranes were placed on new YPL plates supplemented with 50 µg/ml CHX. On day 6, we lysed the yeast cells by placing the membranes on filter paper soaked with colony lysis buffer (0.1% SDS, 0.2 M NaOH, and 0.5% β-mercaptoethanol; Knop et al., 1996). After incubation for 1 h at room temperature, we cleaned the membranes by rinsing off the cell debris with water. The membranes were then subject to HA immunoblotting. The colonies with relatively stronger HA signals were collected onto a new plate and subsequently reexamined for protein degradation by colony assay and Western blot. Finally, the insertion sites were mapped using the Vectorette PCR method (Riley et al., 1990).

Yeast WCE preparation

Cell pellets were resuspended in 300 µl yeast lysis buffer (50 mM NaCl, 50 mM NaF, 100 mM Tris-HCl, pH 7.5, 1 mM EDTA, 1 mM EGTA, 1% Triton X-100, 10% glycerol, 14 mM 2-mercaptoethanol, 2 mM PMSF, 5 µM pepstatin A, and 10 µM leupeptin). After adding ∼80 µl of glass beads, cells were lysed via three rounds of bead-beating (40 s of beating followed by 1 min of cooling on ice). For the degradation assay, cycloheximide was used at 50 µg/ml and MG132 was used at 20 µM.

Yeast IP

Approximately 100–600 ml of cells grown in SCD media to late log phase (OD ∼4) was harvested, flash frozen with liquid nitrogen, and stored at −80°C until cell lysis. Cell pellets were then thawed on ice and resuspended with 2–5 ml yeast lysis buffer. Cells were lysed by nine rounds of bead-beating (20 s beating followed by 1 min of cooling on ice). The crude cell extracts were subject to centrifugation (17,000 *g*) for 10 min at 4°C. The supernatant was then diluted with 3–4 volumes of yeast lysis buffer, mixed with 8–20 µl anti-FLAG or anti-HA agarose beads (Sigma-Aldrich), and incubated at 4°C for 5–6 h (anti-FLAG) or 8–18 h (anti-HA). The agarose beads were then washed four times with yeast lysis buffer and eluted overnight with FLAG or HA peptide (ChinaPeptides Co. Ltd.) at 4°C.

Isolation of the mitochondria-enriched fraction and analysis of submitochondrial localization

Mitochondria were isolated using a previously described method (Diekert et al., 2001), with some modifications. In brief, ∼200 ml cells grown in SCD media to late log phase (OD ∼3) was collected. Cells were washed once with water and incubated in TD buffer (10 mM DTT and 100 mM Tris-SO_4, pH 9.4) for 15 min at 30°C. Cells were then washed once with SP buffer (1.2 M sorbitol and 20 mM potassium phosphate, pH 7.4) and treated with Zymolyase 20T/100T (MP Biomedicals) for 40 min at 30°C to generate spheroplasts. After two washes with SP buffer, the spheroplasts were resuspended in SHE buffer (0.6 M sorbitol, 20 mM Hepes-KOH, pH 7.4, 1 mM EGTA, pH 8, and 2 mM $MgCl_2$) supplemented with protease inhibitors and homogenized in a glass homogenizer (15 strokes). A small aliquot of spheroplasts was saved for making WCEs. The mitochondria-enriched fraction and PMS were obtained by differential centrifugation. Equal amount of proteins from different fractions was analyzed by Western blot.

To determine the submitochondrial localization of proteins, mitochondria were washed twice with SHE buffer and resuspended in isotonic SHE buffer or hypotonic buffer (20 mM Hepes-KOH, pH 7.4)

to ∼1.5–2 mg/ml. Proteinase K (Sigma-Aldrich) was then added to 25 µg/ml and incubated for 20 min on ice. The digestion was stopped by adding TCA to 12% (wt/vol). For alkaline extraction, mitochondria were resuspended in control SHE buffer or sodium carbonate (0.1 M) to ∼1 mg/ml, incubated for 30 min on ice, and then subject to ultracentrifugation (100,000 *g* for 20 min) to obtain the supernatant (soluble proteins) and pellet (insoluble proteins) fractions. Proteins from both fractions were precipitated with 12% TCA. The precipitated proteins were washed once with 5% TCA and once with 100% ethanol and then solubilized in 120 µl of solubilization buffer (40 µl 1 M Tris-HCL, pH 8.0, and 80 µl 2× sample buffer). An equal amount of samples from different treatments was analyzed by Western blot.

Microscopy

Yeast cells were grown in appropriate media (SCD media for Figs. 2 F, 6 F, S1 F, and S3 C; YPL media for Fig. S3 A) to log phase, concentrated, and immobilized on microscope slides. Fluorescent images were captured at 25°C using a 100× objective (CFI Plan Apochromat Lambda, NA 1.45; Nikon) with immersion oil (type NF) on an inverted fluorescence microscope (Eclipse Ti-E; Nikon) with a spinning-disk confocal scanner unit (UltraView; PerkinElmer) with 488 (emission filter 525 [W50]) and 561 (dual-band emission filter 445 [W60] and 615 [W70]) lasers. Z-stack images with 0.5-µm increments were acquired with Volocity software (PerkinElmer) and processed with Volocity and ImageJ software.

Statistical analysis

Data were processed in Excel and analyzed in GraphPad Prism software using the statistical methods as indicated in the figure legends.

Online supplemental material

Fig. S1 provides further characterization of MOM protein degradation and shows the effect of C-terminal tagging on protein localization and cell growth. Fig. S2 shows the development of the genetic screen assay, functional verification of the screen hits, and additional function studies on Doa1. Fig. S3 shows the effect of *DOA1* deletion on mitochondrial morphology and ERMES. Fig. S4 analyzes the submitochondrial localization of Doa1-GFP and the subcellular localization of Ufd1-FLAG in WT and *cdc48-3* cells, and it shows the control data indicating that GFP tagging of Doa1 does not affect MAD. Fig. S5 shows the effect of *DOA1* deletion on the degradation of nonmitochondrial Cdc48 substrates and provides additional synthetic growth analyses between *DOA1* and other mitochondrial quality-control genes. Table S1 summarizes the MOM proteins analyzed in this study and their references. Table S2 summarizes the screen hits of the genetic screen for MAD regulators. Tables S3 and S4 list the strains and plasmids used in this study, respectively. Supplemental references lists the references cited in Table S1 and Fig. S1. Online supplemental material is available at http://www.jcb.org/cgi/content/full/jcb.201510098/DC1.

Acknowledgments

We thank Dr. Xiaodong Wang for discussion and comments and Dr. Benjamin Tufor strains and plasmids.

The research is supported by the National Basic Research Program of China 973 (program 2012CB837503) and the municipal government of Beijing.

The authors declare no competing financial interests.

Submitted: 25 October 2015
Accepted: 2 March 2016

References

Alexandru, G., J. Graumann, G.T. Smith, N.J. Kolawa, R. Fang, and R.J. Deshaies. 2008. UBXD7 binds multiple ubiquitin ligases and implicates p97 in HIF1alpha turnover. *Cell.* 134:804–816. http://dx.doi.org/10.1016/j.cell.2008.06.048

Anton, F., J.M. Fres, A. Schauss, B. Pinson, G.J. Praefcke, T. Langer, and M. Escobar-Henriques. 2011. Ugo1 and Mdm30 act sequentially during Fzo1-mediated mitochondrial outer membrane fusion. *J. Cell Sci.* 124:1126–1135. http://dx.doi.org/10.1242/jcs.073080

Arlt, H., R. Tauer, H. Feldmann, W. Neupert, and T. Langer. 1996. The YTA10-12 complex, an AAA protease with chaperone-like activity in the inner membrane of mitochondria. *Cell.* 85:875–885. http://dx.doi.org/10.1016/S0092-8674(00)81271-4

Baek, G.H., H. Cheng, V. Choe, X. Bao, J. Shao, S. Luo, and H. Rao. 2013. Cdc48: a swiss army knife of cell biology. *J. Amino Acids.* 2013:183421. http://dx.doi.org/10.1155/2013/183421

Bartolome, F., H.-C. Wu, V.S. Burchell, E. Preza, S. Wray, C.J. Mahoney, N.C. Fox, A. Calvo, A. Canosa, C. Moglia, et al. 2013. Pathogenic VCP mutations induce mitochondrial uncoupling and reduced ATP levels. *Neuron.* 78:57–64. http://dx.doi.org/10.1016/j.neuron.2013.02.028

Bebeacua, C., A. Förster, C. McKeown, H.H. Meyer, X. Zhang, and P.S. Freemont. 2012. Distinct conformations of the protein complex p97-Ufd1-Npl4 revealed by electron cryomicroscopy. *Proc. Natl. Acad. Sci. USA.* 109:1098–1103. http://dx.doi.org/10.1073/pnas.1114341109

Beuron, F., I. Dreveny, X. Yuan, V.E. Pye, C. McKeown, L.C. Briggs, M.J. Cliff, Y. Kaneko, R. Wallis, R.L. Isaacson, et al. 2006. Conformational changes in the AAA ATPase p97-p47 adaptor complex. *EMBO J.* 25:1967–1976. http://dx.doi.org/10.1038/sj.emboj.7601055

Braun, R.J., H. Zischka, F. Madeo, T. Eisenberg, S. Wissing, S. Büttner, S.M. Engelhardt, D. Büringer, and M. Ueffing. 2006. Crucial mitochondrial impairment upon CDC48 mutation in apoptotic yeast. *J. Biol. Chem.* 281:25757–25767. http://dx.doi.org/10.1074/jbc.M513699200

Buchberger, A. 2013. Roles of Cdc48 in regulated protein degradation in yeast. *Subcell. Biochem.* 66:195–222. http://dx.doi.org/10.1007/978-94-007-5940-4_8

Burns, N., B. Grimwade, P.B. Ross-Macdonald, E.Y. Choi, K. Finberg, G.S. Roeder, and M. Snyder. 1994. Large-scale analysis of gene expression, protein localization, and gene disruption in Saccharomyces cerevisiae. *Genes Dev.* 8:1087–1105. http://dx.doi.org/10.1101/gad.8.9.1087

Chang, Y.-C., W.-T. Hung, Y.-C. Chang, H.C. Chang, C.-L. Wu, A.-S. Chiang, G.R. Jackson, and T.-K. Sang. 2011. Pathogenic VCP/TER94 alleles are dominant actives and contribute to neurodegeneration by altering cellular ATP level in a Drosophila IBMPFD model. *PLoS Genet.* 7:e1001288. http://dx.doi.org/10.1371/journal.pgen.1001288

Chen, Y.C., G.K. Umanah, N. Dephoure, S.A. Andrabi, S.P. Gygi, T.M. Dawson, V.L. Dawson, and J. Rutter. 2014. Msp1/ATAD1 maintains mitochondrial function by facilitating the degradation of mislocalized tail-anchored proteins. *EMBO J.* 33:1548–1564. http://dx.doi.org/10.15252/embj.201487943

Christianson, T.W., R.S. Sikorski, M. Dante, J.H. Shero, and P. Hieter. 1992. Multifunctional yeast high-copy-number shuttle vectors. *Gene.* 110:119–122. http://dx.doi.org/10.1016/0378-1119(92)90454-W

Cohen, M.M.J., G.P. Leboucher, N. Livnat-Levanon, M.H. Glickman, and A.M. Weissman. 2008. Ubiquitin-proteasome-dependent degradation of a mitofusin, a critical regulator of mitochondrial fusion. *Mol. Biol. Cell.* 19:2457–2464. http://dx.doi.org/10.1091/mbc.E08-02-0227

Collins, Y., E.T. Chouchani, A.M. James, K.E. Menger, H.M. Cochemé, and M.P. Murphy. 2012. Mitochondrial redox signalling at a glance. *J. Cell Sci.* 125:801–806. http://dx.doi.org/10.1242/jcs.098475

Cox, J.S., C.E. Shamu, and P. Walter. 1993. Transcriptional induction of genes encoding endoplasmic reticulum resident proteins requires a transmembrane protein kinase. *Cell.* 73:1197–1206. http://dx.doi.org/10.1016/0092-8674(93)90648-A

Custer, S.K., M. Neumann, H. Lu, A.C. Wright, and J.P. Taylor. 2010. Transgenic mice expressing mutant forms VCP/p97 recapitulate the full spectrum of IBMPFD including degeneration in muscle, brain and bone. *Hum. Mol. Genet.* 19:1741–1755. http://dx.doi.org/10.1093/hmg/ddq050

Diekert, K., A.I. de Kroon, G. Kispal, and R. Lill. 2001. Isolation and subfractionation of mitochondria from the yeast Saccharomyces cerevisiae. *Methods Cell Biol.* 65:37–51. http://dx.doi.org/10.1016/S0091-679X(01)65003-9

Esaki, M., and T. Ogura. 2012. Cdc48p/p97-mediated regulation of mitochondrial morphology is Vms1p-independent. *J. Struct. Biol.* 179:112–120. http://dx.doi.org/10.1016/j.jsb.2012.04.017

Friedlander, R., E. Jarosch, J. Urban, C. Volkwein, and T. Sommer. 2000. A regulatory link between ER-associated protein degradation and the unfolded-protein response. *Nat. Cell Biol.* 2:379–384. http://dx.doi.org/10.1038/35017001

Fu, Q.-S., C.-J. Zhou, H.-C. Gao, Y.-J. Jiang, Z.-R. Zhou, J. Hong, W.-M. Yao, A.-X. Song, D.-H. Lin, and H.-Y. Hu. 2009. Structural basis for ubiquitin recognition by a novel domain from human phospholipase A2-activating protein. *J. Biol. Chem.* 284:19043–19052. http://dx.doi.org/10.1074/jbc.M109.009126

Ghislain, M., R.J. Dohmen, F. Levy, and A. Varshavsky. 1996. Cdc48p interacts with Ufd3p, a WD repeat protein required for ubiquitin-mediated proteolysis in Saccharomyces cerevisiae. *EMBO J.* 15:4884–4899.

Gibson, D.G., L. Young, R.Y. Chuang, J.C. Venter, C.A. Hutchison III, and H.O. Smith. 2009. Enzymatic assembly of DNA molecules up to several hundred kilobases. *Nat. Methods.* 6:343–345. http://dx.doi.org/10.1038/nmeth.1318

Griffin, E.E., and D.C. Chan. 2006. Domain interactions within Fzo1 oligomers are essential for mitochondrial fusion. *J. Biol. Chem.* 281:16599–16606. http://dx.doi.org/10.1074/jbc.M601847200

Hampton, R.Y., R.G. Gardner, and J. Rine. 1996. Role of 26S proteasome and HRD genes in the degradation of 3-hydroxy-3-methylglutaryl-CoA reductase, an integral endoplasmic reticulum membrane protein. *Mol. Biol. Cell.* 7:2029–2044. http://dx.doi.org/10.1091/mbc.7.12.2029

Heo, J.-M., N. Livnat-Levanon, E.B. Taylor, K.T. Jones, N. Dephoure, J. Ring, J. Xie, J.L. Brodsky, F. Madeo, S.P. Gygi, et al. 2010. A stress-responsive system for mitochondrial protein degradation. *Mol. Cell.* 40:465–480. http://dx.doi.org/10.1016/j.molcel.2010.10.021

Hetzer, M., H.H. Meyer, T.C. Walther, D. Bilbao-Cortes, G. Warren, and I.W. Mattaj. 2001. Distinct AAA-ATPase p97 complexes function in discrete steps of nuclear assembly. *Nat. Cell Biol.* 3:1086–1091. http://dx.doi.org/10.1038/ncb1201-1086

Hiller, M.M., A. Finger, M. Schweiger, and D.H. Wolf. 1996. ER degradation of a misfolded luminal protein by the cytosolic ubiquitin-proteasome pathway. *Science.* 273:1725–1728. http://dx.doi.org/10.1126/science.273.5282.1725

Hirsch, C., R. Gauss, S.C. Horn, O. Neuber, and T. Sommer. 2009. The ubiquitylation machinery of the endoplasmic reticulum. *Nature.* 458:453–460. http://dx.doi.org/10.1038/nature07962

Huibregtse, J.M., M. Scheffner, S. Beaudenon, and P.M. Howley. 1995. A family of proteins structurally and functionally related to the E6-AP ubiquitin-protein ligase. *Proc. Natl. Acad. Sci. USA.* 92:2563–2567. http://dx.doi.org/10.1073/pnas.92.7.2563

Janke, C., M.M. Magiera, N. Rathfelder, C. Taxis, S. Reber, H. Maekawa, A. Moreno-Borchart, G. Doenges, E. Schwob, E. Schiebel, and M. Knop. 2004. A versatile toolbox for PCR-based tagging of yeast genes: new fluorescent proteins, more markers and promoter substitution cassettes. *Yeast.* 21:947–962. http://dx.doi.org/10.1002/yea.1142

Jarosch, E., C. Taxis, C. Volkwein, J. Bordallo, D. Finley, D.H. Wolf, and T. Sommer. 2002. Protein dislocation from the ER requires polyubiquitination and the AAA-ATPase Cdc48. *Nat. Cell Biol.* 4:134–139. http://dx.doi.org/10.1038/ncb746

Johnson, E.S., P.C.M. Ma, I.M. Ota, and A. Varshavsky. 1995. A proteolytic pathway that recognizes ubiquitin as a degradation signal. *J. Biol. Chem.* 270:17442–17456. http://dx.doi.org/10.1074/jbc.270.29.17442

Johnson, J.O., J. Mandrioli, M. Benatar, Y. Abramzon, V.M. Van Deerlin, J.Q. Trojanowski, J.R. Gibbs, M. Brunetti, S. Gronka, J. Wuu, et al. ITA LSGEN Consortium. 2010. Exome sequencing reveals VCP mutations as a cause of familial ALS. *Neuron.* 68:857–864. http://dx.doi.org/10.1016/j.neuron.2010.11.036

Kanki, T., K. Wang, Y. Cao, M. Baba, and D.J. Klionsky. 2009. Atg32 is a mitochondrial protein that confers selectivity during mitophagy. *Dev. Cell.* 17:98–109. http://dx.doi.org/10.1016/j.devcel.2009.06.014

Karbowski, M., and R.J. Youle. 2011. Regulating mitochondrial outer membrane proteins by ubiquitination and proteasomal degradation. *Curr. Opin. Cell Biol.* 23:476–482. http://dx.doi.org/10.1016/j.ceb.2011.05.007

Kim, N.C., E. Tresse, R.M. Kolaitis, A. Molliex, R.E. Thomas, N.H. Alami, B. Wang, A. Joshi, R.B. Smith, G.P. Ritson, et al. 2013. VCP is essential for mitochondrial quality control by PINK1/Parkin and this function is impaired by VCP mutations. *Neuron.* 78:65–80. (published erratum appears in *Neuron*. 78:403) http://dx.doi.org/10.1016/j.neuron.2013.02.029

Knop, M., A. Finger, T. Braun, K. Hellmuth, and D.H. Wolf. 1996. Der1, a novel protein specifically required for endoplasmic reticulum degradation in yeast. *EMBO J.* 15:753–763.

Koegl, M., T. Hoppe, S. Schlenker, H.D. Ulrich, T.U. Mayer, and S. Jentsch. 1999. A novel ubiquitination factor, E4, is involved in multiubiquitin chain assembly. *Cell.* 96:635–644. http://dx.doi.org/10.1016/S0092-8674(00)80574-7

Kornmann, B., E. Currie, S.R. Collins, M. Schuldiner, J. Nunnari, J.S. Weissman, and P. Walter. 2009. An ER-mitochondria tethering complex revealed by a synthetic biology screen. *Science.* 325:477–481. http://dx.doi.org/10.1126/science.1175088

Longtine, M.S., A. McKenzie III, D.J. Demarini, N.G. Shah, A. Wach, A. Brachat, P. Philippsen, and J.R. Pringle. 1998. Additional modules for versatile and economical PCR-based gene deletion and modification in Saccharomyces cerevisiae. *Yeast.* 14:953–961. http://dx.doi.org/10.1002/(SICI)1097-0061(199807)14:10<953::AID-YEA293>3.0.CO;2-U

Luhtala, N., and G. Odorizzi. 2004. Bro1 coordinates deubiquitination in the multivesicular body pathway by recruiting Doa4 to endosomes. *J. Cell Biol.* 166:717–729. http://dx.doi.org/10.1083/jcb.200403139

Meyer, H., M. Bug, and S. Bremer. 2012. Emerging functions of the VCP/p97 AAA-ATPase in the ubiquitin system. *Nat. Cell Biol.* 14:117–123. http://dx.doi.org/10.1038/ncb2407

Meyer, H.H., Y. Wang, and G. Warren. 2002. Direct binding of ubiquitin conjugates by the mammalian p97 adaptor complexes, p47 and Ufd1-Npl4. *EMBO J.* 21:5645–5652. http://dx.doi.org/10.1093/emboj/cdf579

Mullally, J.E., T. Chernova, and K.D. Wilkinson. 2006. Doa1 is a Cdc48 adapter that possesses a novel ubiquitin binding domain. *Mol. Cell. Biol.* 26:822–830. http://dx.doi.org/10.1128/MCB.26.3.822-830.2006

Nakatsukasa, K., J.L. Brodsky, and T. Kamura. 2013. A stalled retrotranslocation complex reveals physical linkage between substrate recognition and proteasomal degradation during ER-associated degradation. *Mol. Biol. Cell.* 24:1765–1775: S1–S8. http://dx.doi.org/10.1091/mbc.E12-12-0907

Nalbandian, A., K.J. Llewellyn, M. Kitazawa, H.Z. Yin, M. Badadani, N. Khanlou, R. Edwards, C. Nguyen, J. Mukherjee, T. Mozaffar, et al. 2012. The homozygote $VCP^{R155H/R155H}$ mouse model exhibits accelerated human VCP-associated disease pathology. *PLoS One.* 7:e46308. http://dx.doi.org/10.1371/journal.pone.0046308

Neuber, O., E. Jarosch, C. Volkwein, J. Walter, and T. Sommer. 2005. Ubx2 links the Cdc48 complex to ER-associated protein degradation. *Nat. Cell Biol.* 7:993–998. http://dx.doi.org/10.1038/ncb1298

Ng, D.T., E.D. Spear, and P. Walter. 2000. The unfolded protein response regulates multiple aspects of secretory and membrane protein biogenesis and endoplasmic reticulum quality control. *J. Cell Biol.* 150:77–88. http://dx.doi.org/10.1083/jcb.150.1.77

Nishimasu, R., H. Komori, Y. Higuchi, H. Nishimasu, and H. Hiroaki. 2010. Crystal structure of a PFU-PUL domain pair of Saccharomyces cerevisiae Doa1/Ufd3. *Kobe J. Med. Sci.* 56:E125–E139.

Okamoto, K., N. Kondo-Okamoto, and Y. Ohsumi. 2009. Mitochondria-anchored receptor Atg32 mediates degradation of mitochondria via selective autophagy. *Dev. Cell.* 17:87–97. http://dx.doi.org/10.1016/j.devcel.2009.06.013

Okreglak, V., and P. Walter. 2014. The conserved AAA-ATPase Msp1 confers organelle specificity to tail-anchored proteins. *Proc. Natl. Acad. Sci. USA.* 111:8019–8024. http://dx.doi.org/10.1073/pnas.1405755111

Pashkova, N., L. Gakhar, S.C. Winistorfer, L. Yu, S. Ramaswamy, and R.C. Piper. 2010. WD40 repeat propellers define a ubiquitin-binding domain that regulates turnover of F box proteins. *Mol. Cell.* 40:433–443. http://dx.doi.org/10.1016/j.molcel.2010.10.018

Pye, V.E., F. Beuron, C.A. Keetch, C. McKeown, C.V. Robinson, H.H. Meyer, X. Zhang, and P.S. Freemont. 2007. Structural insights into the p97-Ufd1-Npl4 complex. *Proc. Natl. Acad. Sci. USA.* 104:467–472. http://dx.doi.org/10.1073/pnas.0603408104

Qiu, L., N. Pashkova, J.R. Walker, S. Winistorfer, A. Allali-Hassani, M. Akutsu, R. Piper, and S. Dhe-Paganon. 2010. Structure and function of the PLAA/Ufd3-p97/Cdc48 complex. *J. Biol. Chem.* 285:365–372. http://dx.doi.org/10.1074/jbc.M109.044685

Quirós, P.M., T. Langer, and C. López-Otín. 2015. New roles for mitochondrial proteases in health, ageing and disease. *Nat. Rev. Mol. Cell Biol.* 16:345–359. http://dx.doi.org/10.1038/nrm3984

Rapaport, D., M. Brunner, W. Neupert, and B. Westermann. 1998. Fzo1p is a mitochondrial outer membrane protein essential for the biogenesis of functional mitochondria in Saccharomyces cerevisiae. *J. Biol. Chem.* 273:20150–20155. http://dx.doi.org/10.1074/jbc.273.32.20150

Riley, J., R. Butler, D. Ogilvie, R. Finniear, D. Jenner, S. Powell, R. Anand, J.C. Smith, and A.F. Markham. 1990. A novel, rapid method for the isolation of terminal sequences from yeast artificial chromosome (YAC) clones. *Nucleic Acids Res.* 18:2887–2890. http://dx.doi.org/10.1093/nar/18.10.2887

Rotin, D., and S. Kumar. 2009. Physiological functions of the HECT family of ubiquitin ligases. *Nat. Rev. Mol. Cell Biol.* 10:398–409. http://dx.doi.org/10.1038/nrm2690

Rumpf, S., and S. Jentsch. 2006. Functional division of substrate processing cofactors of the ubiquitin-selective Cdc48 chaperone. *Mol. Cell.* 21:261–269. http://dx.doi.org/10.1016/j.molcel.2005.12.014

Schuberth, C., and A. Buchberger. 2005. Membrane-bound Ubx2 recruits Cdc48 to ubiquitin ligases and their substrates to ensure efficient ER-associated protein degradation. *Nat. Cell Biol.* 7:999–1006. http://dx.doi.org/10.1038/ncb1299

Shcherbik, N., and D.S. Haines. 2007. Cdc48p(Npl4p/Ufd1p) binds and segregates membrane-anchored/tethered complexes via a polyubiquitin signal present on the anchors. *Mol. Cell.* 25:385–397. http://dx.doi.org/10.1016/j.molcel.2007.01.024

Sherman, F. 2002. Getting started with yeast. *Methods Enzymol.* 350:3–41. http://dx.doi.org/10.1016/S0076-6879(02)50954-X

Stolz, A., W. Hilt, A. Buchberger, and D.H. Wolf. 2011. Cdc48: a power machine in protein degradation. *Trends Biochem. Sci.* 36:515–523. http://dx.doi.org/10.1016/j.tibs.2011.06.001

Suzuki, C.K., K. Suda, N. Wang, and G. Schatz. 1994. Requirement for the yeast gene LON in intramitochondrial proteolysis and maintenance of respiration. *Science.* 264:891. http://dx.doi.org/10.1126/science.8178144

Swanson, R., M. Locher, and M. Hochstrasser. 2001. A conserved ubiquitin ligase of the nuclear envelope/endoplasmic reticulum that functions in both ER-associated and Matalpha2 repressor degradation. *Genes Dev.* 15:2660–2674. http://dx.doi.org/10.1101/gad.933301

Tanaka, A., M.M. Cleland, S. Xu, D.P. Narendra, D.-F. Suen, M. Karbowski, and R.J. Youle. 2010. Proteasome and p97 mediate mitophagy and degradation of mitofusins induced by Parkin. *J. Cell Biol.* 191:1367–1380. http://dx.doi.org/10.1083/jcb.201007013

Taxis, C., and M. Knop. 2006. System of centromeric, episomal, and integrative vectors based on drug resistance markers for Saccharomyces cerevisiae. *Biotechniques.* 40:73–78. http://dx.doi.org/10.2144/000112040

Taylor, E.B., and J. Rutter. 2011. Mitochondrial quality control by the ubiquitin-proteasome system. *Biochem. Soc. Trans.* 39:1509–1513. http://dx.doi.org/10.1042/BST0391509

van Dijken, J.P., J. Bauer, L. Brambilla, P. Duboc, J.M. Francois, C. Gancedo, M.L. Giuseppin, J.J. Heijnen, M. Hoare, H.C. Lange, E.A. Madden, et al. 2000. An interlaboratory comparison of physiological and genetic properties of four *Saccharomyces cerevisiae* strains. *Enzyme Microb. Technol.* 26:706–714. http://dx.doi.org/10.1016/S0141-0229(00)00162-9

Van Dyck, L., D.A. Pearce, and F. Sherman. 1994. PIM1 encodes a mitochondrial ATP-dependent protease that is required for mitochondrial function in the yeast Saccharomyces cerevisiae. *J. Biol. Chem.* 269:238–242.

van Loon, A.P., B. Pesold-Hurt, and G. Schatz. 1986. A yeast mutant lacking mitochondrial manganese-superoxide dismutase is hypersensitive to oxygen. *Proc. Natl. Acad. Sci. USA.* 83:3820–3824. http://dx.doi.org/10.1073/pnas.83.11.3820

Verma, R., S. Chen, R. Feldman, D. Schieltz, J. Yates, J. Dohmen, and R.J. Deshaies. 2000. Proteasomal proteomics: identification of nucleotide-sensitive proteasome-interacting proteins by mass spectrometric analysis of affinity-purified proteasomes. *Mol. Biol. Cell.* 11:3425–3439. http://dx.doi.org/10.1091/mbc.11.10.3425

Verma, R., R. Oania, R. Fang, G.T. Smith, and R.J. Deshaies. 2011. Cdc48/p97 mediates UV-dependent turnover of RNA Pol II. *Mol. Cell.* 41:82–92. http://dx.doi.org/10.1016/j.molcel.2010.12.017

Verma, R., R.S. Oania, N.J. Kolawa, and R.J. Deshaies. 2013. Cdc48/p97 promotes degradation of aberrant nascent polypeptides bound to the ribosome. *eLife.* 2:e00308. http://dx.doi.org/10.7554/eLife.00308

Voth, W.P., J.D. Richards, J.M. Shaw, and D.J. Stillman. 2001. Yeast vectors for integration at the HO locus. *Nucleic Acids Res.* 29:E59–E9. http://dx.doi.org/10.1093/nar/29.12.e59

Walter, J., J. Urban, C. Volkwein, and T. Sommer. 2001. Sec61p-independent degradation of the tail-anchored ER membrane protein Ubc6p. *EMBO J.* 20:3124–3131. http://dx.doi.org/10.1093/emboj/20.12.3124

Watts, G.D.J., J. Wymer, M.J. Kovach, S.G. Mehta, S. Mumm, D. Darvish, A. Pestronk, M.P. Whyte, and V.E. Kimonis. 2004. Inclusion body myopathy associated with Paget disease of bone and frontotemporal dementia is caused by mutant valosin-containing protein. *Nat. Genet.* 36:377–381. http://dx.doi.org/10.1038/ng1332

Wu, X., and B.P. Tu. 2011. Selective regulation of autophagy by the Iml1-Npr2-Npr3 complex in the absence of nitrogen starvation. *Mol. Biol. Cell.* 22:4124–4133. http://dx.doi.org/10.1091/mbc.E11-06-0525

Xu, S., G. Peng, Y. Wang, S. Fang, and M. Karbowski. 2011. The AAA-ATPase p97 is essential for outer mitochondrial membrane protein turnover. *Mol. Biol. Cell.* 22:291–300. http://dx.doi.org/10.1091/mbc.E10-09-0748

Ye, Y., H.H. Meyer, and T.A. Rapoport. 2001. The AAA ATPase Cdc48/p97 and its partners transport proteins from the ER into the cytosol. *Nature.* 414:652–656. http://dx.doi.org/10.1038/414652a

Ye, Y., H.H. Meyer, and T.A. Rapoport. 2003. Function of the p97-Ufd1-Npl4 complex in retrotranslocation from the ER to the cytosol: dual recognition of nonubiquitinated polypeptide segments and polyubiquitin chains. *J. Cell Biol.* 162:71–84. http://dx.doi.org/10.1083/jcb.200302169

Yin, H.Z., A. Nalbandian, C.I. Hsu, S. Li, K.J. Llewellyn, T. Mozaffar, V.E. Kimonis, and J.H. Weiss. 2012. Slow development of ALS-like spinal cord pathology in mutant valosin-containing protein gene knock-in mice. *Cell Death Dis.* 3:e374. http://dx.doi.org/10.1038/cddis.2012.115

Youle, R.J., and D.P. Narendra. 2011. Mechanisms of mitophagy. *Nat. Rev. Mol. Cell Biol.* 12:9–14. http://dx.doi.org/10.1038/nrm3028

Zahedi, R.P., A. Sickmann, A.M. Boehm, C. Winkler, N. Zufall, B. Schönfisch, B. Guiard, N. Pfanner, and C. Meisinger. 2006. Proteomic analysis of the yeast mitochondrial outer membrane reveals accumulation of a subclass of preproteins. *Mol. Biol. Cell.* 17:1436–1450. http://dx.doi.org/10.1091/mbc.E05-08-0740

Zhao, G., G. Li, H. Schindelin, and W.J. Lennarz. 2009. An Armadillo motif in Ufd3 interacts with Cdc48 and is involved in ubiquitin homeostasis and protein degradation. *Proc. Natl. Acad. Sci. USA.* 106:16197–16202. http://dx.doi.org/10.1073/pnas.0908321106